NANO · MICRO small
www.small-journal.com

Toward Sustainable and High-Performing Energy Storage from Biomass Waste Through Hydrothermal Carbonization

Hong Duc Pham, Tristan Shelley,* Paulomi (Polly) Burey,* Pratheep Kumar Annamalai, Jessica Feldman, Tan Tien Nguyen, Andreas Helwig, and Ashok Kumar Nanjundan**

The demand for valuable and sustainable chemicals and nonfossil fuels, with a carbon-neutral or zero-carbon footprint from zero-cost, abundant waste streams, has garnered significant interest in recent years. This has been driven by a global desire to transition to a circular economy, by reducing global reliance and eventually the need for fossil-based resources. Hydrothermal carbonization (HTC), a thermal conversion technology, is widely used to recover carbon and energy from waste, avoiding the energy-intensive drying process for high-moisture feedstock, and operating at lower temperatures than conventional processes. The main product, waste-derived hydrochar (WHC), has attracted growing interest in electrochemical energy storage (EES) devices (e.g., rechargeable batteries and supercapacitors) due to its straightforward process, favorable properties, high carbon conversion, and environmental benefits. Hence, this critical review will provide the reader with a better understanding of the principles, technical feasibility, and limitations of carbon conversion from waste through various conversion pathways. Moreover, it presents detailed state-of-the-art studies previously reported on WHC production using one-step direct carbonization (DC) and the two-step HTC followed by DC for electrochemical energy storage applications, with a focus on the role of WHC-based electrodes. Lastly, the challenges and prospects for developing WHC materials for EES applications are examined.

1. Introduction

Traditional carbon materials such as graphene and carbon nanotubes are mainly synthesized using natural gas, a limited fossil fuel resource.[1,2] They are being widely applied as promising materials for various applications, such as energy storage devices.[3,4] Nevertheless, their excessive use results in a heavy reliance on fossil fuel sources, contributing to consequences such as exacerbating the effects of greenhouse gas emissions and their impacts on climate change. Apart from the demand for reducing the reliance on fossil fuels, the ongoing issue of abundant waste and a shortage of natural resources are receiving considerable attention. Hence, it is timely and appropriate to explore newly developed energy technologies that are environmentally friendly, ensuring the sustainable future of human society.

Waste is widely distributed and abundant in the world. For instance, roughly 10–15 billion tons of waste are generated yearly worldwide, which are generally disposed of in landfills or by direct combustion, resulting in significant environmental pollution.[5] Instead of being disposed of, waste can serve as a zero-cost feedstock for promoting sustainable development, and it further saves the costs of landfill levies for many organic waste streams, which are imposed in many jurisdictions worldwide. As a carbon sink, the conversion of organic or other industrial wastes to carbon may also potentially participate in current and future global carbon trading schemes, further enhancing the profitability of circular economy endeavors. Indeed, the sustainable development of waste-derived carbonaceous materials has been intensively explored across a wide range

H. D. Pham, T. Shelley, P. (Polly) Burey, P. K. Annamalai, J. Feldman, A. Helwig, A. K. Nanjundan
Centre for Future Materials
University of Southern Queensland
Toowoomba, Queensland 4350, Australia
E-mail: david.pham@unisq.edu.au; Tristan.Shelley@unisq.edu.au; Polly.Burey@unisq.edu.au; Ashok.Nanjundan@unisq.edu.au

The ORCID identification number(s) for the author(s) of this article can be found under https://doi.org/10.1002/smll.202509226

DOI: 10.1002/smll.202509226

P. (Polly) Burey
School of Agriculture and Environmental Science
University of Southern Queensland
Toowoomba, Queensland 4350, Australia

T. T. Nguyen
Key Laboratory of Digital Control and System Engineering (DCSELab)
Faculty of Mechanical Engineering
Ho Chi Minh City University of Technology
Vietnam National University Ho Chi Minh City
Ho Chi Minh City 700000, Vietnam

A. Helwig
School of Engineering
University of Southern Queensland
Toowoomba, Queensland 4350, Australia

A. K. Nanjundan
School of Engineering
University of Southern Queensland
Springfield, Queensland 4300, Australia

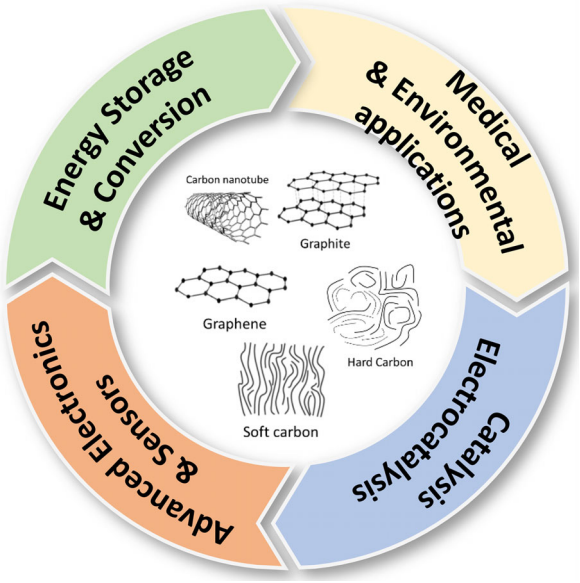

Figure 1. Schematic structures of carbon-based materials and reported relevant applications.

of applications (**Figure 1**), including rechargeable batteries, supercapacitors, sensing devices, and environmental remediation, among others.[5–10]

The construction of rechargeable batteries (e.g., lithium- and sodium-ion batteries (LIBs and SIBs, respectively) and supercapacitors (SCs)) involves carbon-based materials as electrodes, playing a crucial role in their electrochemical performance and efficiency.[11–13] In terms of LIBs, although graphite has been intensively employed in commercial batteries, replacing graphite with other low-cost carbon-based anodes is emerging due to price competition with SIBs, the tedious process of graphite synthesis, and the need for a sustainable strategy. While upcycling spent graphite from end-of-life LIBs has been explored,[14] the impurities in graphite after a thousand charging and discharging cycles may require further purification treatment, thereby increasing the production costs. Additionally, the use of impure spent graphite may compromise the quality of the reused batteries. For SIBs anodes, carbon-based materials (e.g., hard carbon, soft carbon, and graphite) and non-carbon-based ones (e.g., metal alloy materials, titanium compounds, organic molecules, and metal-based composites) have been widely investigated and developed.[15–17] Although non-carbon anodes have offered higher theoretical capacities, they have suffered from electrode swelling and a tedious multi-step synthesis process.[18] In contrast, carbon-based materials derived from biomass waste are easy and inexpensive to produce. Remarkably, their manufacturing process can be expanded for large-scale production. Because their structure remains largely unchanged during the insertion and removal of sodium ions, the stability of the battery can be improved.[15,18–20] SCs have suffered from low energy density and high production costs. To address this, carbon-based electrodes have been intensively studied in SCs to enhance energy density. Specifically, synthesizing carbon-based electrodes derived from zero-cost waste has offered a cost-effective solution.[11,21,22] Overall, the pursuit of developing waste-derived carbonaceous electrodes for next-generation energy storage systems is both urgent and timely, owing to their environmental advantages, low-cost production, and sustainability.

There are several methods for converting waste into energy. Among them, thermal conversion technologies (e.g., combustion, pyrolysis, and gasification) have been widely utilized to recover energy and carbon from waste-based feedstocks due to their simple processes and wide availability.[23] However, they have faced several challenges with conventional thermal conversion methods, including high moisture content, drying and preprocessing requirements, and high energy input. To mitigate, several studies related to hydrothermal carbonization (HTC) have been increasingly viewed as a key solution to enhance carbon recovery, as well as improve the efficiency and scalability of waste-derived carbonaceous materials.[7,8,24–27] HTC is one of the thermochemical processes that produces hydrochar (WHC), as well as liquid and gaseous products. HTC typically emphasizes its potential as a promising technology because it offers several benefits: 1) it avoids the energy-intensive drying process required for high-moisture feedstock; 2) its operating temperatures (below 250 °C) are much lower than conventional thermal conversion of biomass; 3) the WHC yield (50%) and energy recovery (80%) is high; 4) the circular bioeconomy can be established when HTC is integrated with anaerobic digestion to utilize the downstream liquid waste of HTC.[25,28]

HTC has previously been shown to play a pivotal role in synthesizing sustainable HC, the main product, for diverse applications due to its low cost, high carbon conversion efficiency, greenness, and simplicity. Notably, the introduction of the sustainable circular economy based on WHC in electrochemical energy storage devices using waste-derived carbon electrodes has led to a growing number of studies.[29,30] HTC, followed by one-step direct carbonization (DC) (denoted as HTC-DC), provided a favorable quality of carbon-based electrodes, leading to higher capacity and longer cycling ability than the traditional one-step DC under identical electrochemical characterization.[24] The two-step HTC-DC method also offers further sustainability, carbon neutrality, and higher carbon recovery compared to the one-step DC.[29] Additionally, the fibrous porous carbon network is formed in HTC-DC, while this observation was not found in DC.[31] A cascaded HTC-DC also promotes pore enlargement and the creation of nanosphere domains, enhancing the electrochemical reversible capacity.[32]

This review systematically provides a comprehensive overview of waste-derived carbonaceous electrodes used in emerging applications such as rechargeable metal-ion batteries and supercapacitors (SCs). It covers the applications of rechargeable batteries (e.g., LIBs and SIBs) and SCs through one-step DC and two-step HTC-DC processes. The review also examines the advantages and disadvantages of the two-step pathway, with particular focus on the role of HTC, which has been less explored in the literature. Finally, it discusses opportunities, challenges, and strategies for improving carbon electrode materials in energy storage devices, supporting the move toward large-scale commercialization of waste-heat carbon (WHC).

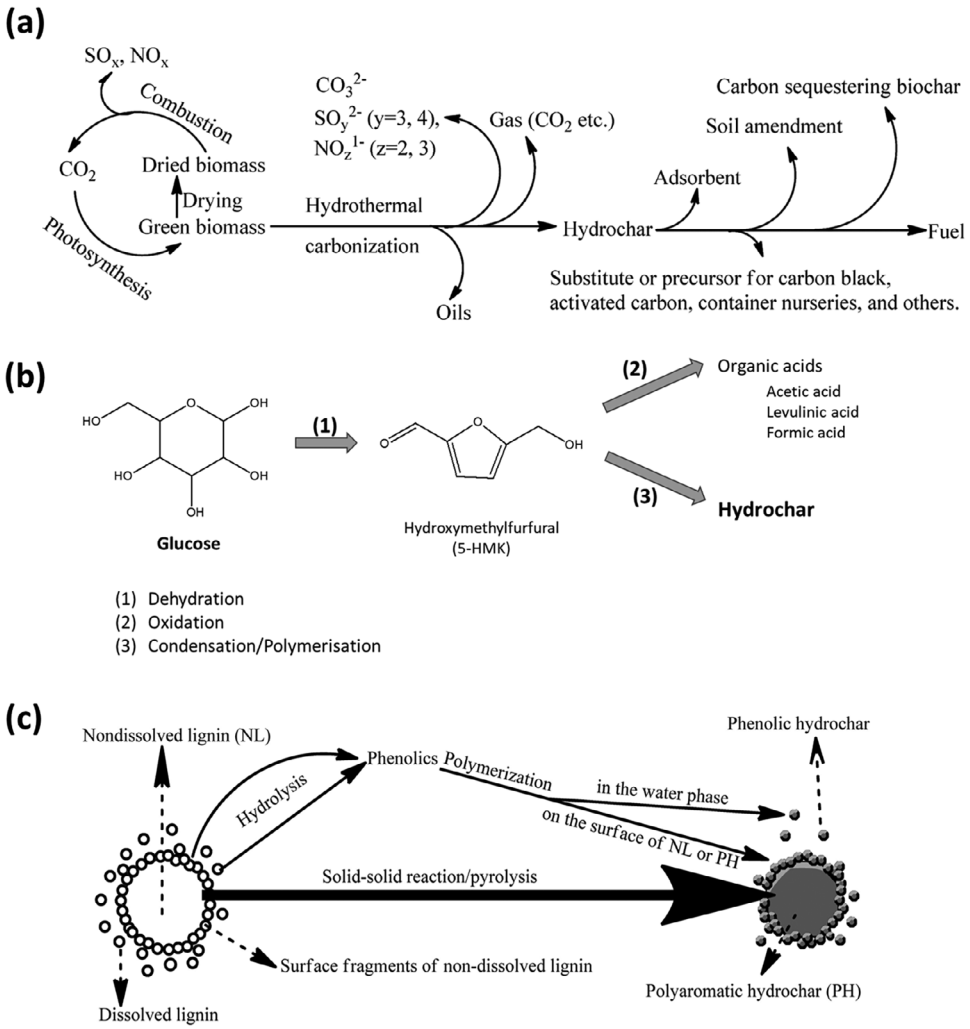

Figure 2. a) The objectives and potential applications of biomass HTC. Reproduced with permission.[34] Copyright 2025, American Chemical Society. b) Simplified reaction pathway of glucose transformation into HTC hydrochar.[35,36] (c) Proposed formation pathways of lignin-derived hydrochar HTC. Reproduced with permission.[34] Copyright 2025, American Chemical Society.

2. Hydrothermal Carbonization

2.1. Fundamentals and Reaction Mechanisms

The HTC process has been widely used to transform either high-moisture-containing feedstocks (e.g., sludge and municipal waste) or low-moisture ones (e.g., lignocellulosic biomass) into homogeneous carbon-rich material (known as WHC), aqueous compounds, and gaseous streams (mainly CO_2).[33] WHC (or hydrochar, as shown in **Figure 2**a) has multiple applications, including soil amendment, adsorbent for mitigating pollutants, carbon sequestration as biochar, and as a fuel source. The emission of gases, such as CO_2, NO_z^{1-} etc., re-enter the carbon cycle, where they are utilized by plants for photosynthesis, contributing to biomass growth.

Essentially, the optimized WHC yield depends on the choice of the feedstock, temperature, residence time, and the feedstock-to-water ratio.[37,38] The feedstock composition (e.g., lignocellulosic, sludge) influences hydrochar properties; for example, a high lignin content in the feedstock results in higher WHC yields.[39] The type of feedstock also influences the feedstock-to-water ratio. As in earlier attempts, a ratio between 1:5 and 1:10 ensures sufficient moisture for reactions while maintaining process efficiency. For operating temperatures (typically ranging from 180 to 250 °C), higher temperatures not only enhance carbonization yield but also potentially reduce WHC yield. The HTC yield may be reduced if the residence time is excessive.

In HTC, water is used as the most environmentally friendly solvent. It serves as a reactant and an effective medium for acid-catalysed reactions, leveraging the high H^+ ion concentration from subcritical water to break down biomass into smaller fractions. The main reactions in HTC are hydrolysis, dehydration, decarboxylation, polymerization, recondensation, aromatization, and Maillard reactions.[37]

Due to the water-mediated solvent and wet feedstock, HTC has potential for economic and energy benefits.[37] Process water (PW) is the by-product of the HTC process. Antonio and co-authors found that replacing deionized water with recycled PW

Table 1. A comparison of operating conditions and typical carbon-based yield of various thermochemical processes.[41–45]

Method	Operating Temp. [°C]	Residence Time	Yield [%]
Fast pyrolysis	400–550	1 (s)	<15
Intermediate pyrolysis	600–750	10–60 (s)	<20
Slow pyrolysis	300–650	>30 (min)	<35
Gasification	600–900	10–20 (s)	<10
Dry torrefaction	200–350	30–240 (min)	70–80
DC	600–1600	30–120 (min)	<40
HTC	180–250	5–720 (min)	50–80

as an HTC solvent resulted in an eightfold increase in energy recovery. Additionally, the carbon content and energy yield of hydrochar increased by ≈26% and 27%, respectively.[40]

2.2. Conversion of Waste to Carbon

Depending on the feedstock types, the desired properties of carbon materials, and the required applications, various production technologies are available, such as pyrolysis, gasification, DC, and HTC, as summarized in **Table 1**.

In general, it highlights the trade-offs between three primary parameters, including operating temperature (°C), residence time, and carbon yield (%), across these methods. Synthetic methods (e.g., HTC, torrefaction) with moderate working temperatures and long residence times typically yield high carbon content (>50%). Conversely, the yields from other methods, which operate at high temperatures and short reaction times (e.g., pyrolysis and gasification), have been reduced, with liquid and gaseous products being the primary outputs. While the residence time of pyrolysis methods is less energy-intensive, their yields are comparatively low. Dry torrefaction requires dried feedstock and an inert environment during operation. The WHC-based torrefaction has a lower porosity and fewer functional groups compared to the HTC-based WHC.[46] Compared to other processes, the carbon conversion yield using HTC is over 50%, which is higher than that obtained from other methods. HTC also offers lower working temperatures.[41–44] Moreover, the energy and carbon recovery of HTC is far better than others since the drying step is avoidable and the liquid by-product can be recycled for anaerobic digestion and soil amendment.[47]

3. The Role of Waste Hydrochar-Based Electrodes in Electrochemical Energy Storage

While WHC-based electrodes have been studied in other battery chemistries, such as lithium–sulfur[48] and lithium–selenium batteries,[49] LIBs and SIBs are the focus of this review because they are dominant technologies in high-level R&D and commercial production (e.g., electric vehicles and portable electronic devices). In this section, electrodes based on WHC for rechargeable batteries (e.g., LIBs and SIBs) and supercapacitors will be the focus. **Figure 3** illustrates the number of research articles where carbon-based electrodes have been used in LIBs, SIBs, and SCs from 2015 to 2024. Overall, research articles for all devices were relatively few before 2018. Since then, there has been a notable increase across all categories, especially in SCs. Interest in SC studies continued to grow until 2020. By 2022, research on SIBs had become prominent, surpassing both SCs and LIBs. This is consistent with the expansion plans for SIBs by leading battery manufacturers from 2023.[50] Moreover, the significantly increasing demand for lower-cost and safer battery technologies is leading to a potential shift in research priorities toward SIBs.[24] Additionally, there has been considerable advancement in upcycling biomass waste into sustainable battery technologies.[19,44,51]

3.1. Ion Storage Mechanism in Waste-Derived Hard Carbon

Prior to reviewing the state-of-the-art literature on HTC applications for EES, a brief discussion of the electrochemical storage mechanism of alkali-metal ions (e.g., Na^+, K^+, and Li^+) in WHC is provided. Even though this has been investigated intensively, storing these ions in hard carbon has become a topic of debate due to the variation in WHC structures (e.g., diverse precursors, micropore size, defect sites, residual heteroatoms, and so on) and electrochemical testing conditions.[52–58]

In general, alkali-metal ions can be hosted by the expanded, parallel, and curved layers of the graphitic structures in WHC (see **Figure 4**).[59] Depending on the ionic radius (e.g., K^+ (2.27 Å) > Na^+ (1.86 Å) > Li^+ (1.52 Å)),[60] the (002) interlayer spacing of WHC, the stable formation of the intercalation (after these ions are accommodated in graphitic layers), and the resulting device capacity and cycling stability vary. The insertion of Li^+ ions in WHC structures forms a stable Li-intercalated graphite (LiC_6). In terms of Na^+ ions, their intercalation results in two Na-intercalated graphite compounds: NaC_6 and NaC_8, which are thermodynamically unstable. Meanwhile, even though only K-intercalated graphite is established, the K^+ intercalation has suffered because of its largest radius.[60] Since this review focuses on LIBs and SIBs, the chemistry of KIBs is not described.

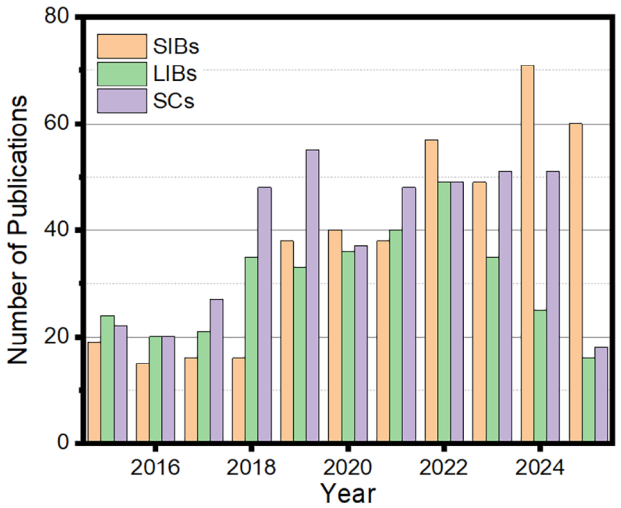

Figure 3. The number of research articles (English version, excluding reviews and conference papers) focusing on carbon-based electrodes for lithium-ion batteries (LIBs), sodium-ion batteries (SIBs), and Supercapacitors (SCs) (SCOPUS accessed on May 2025).

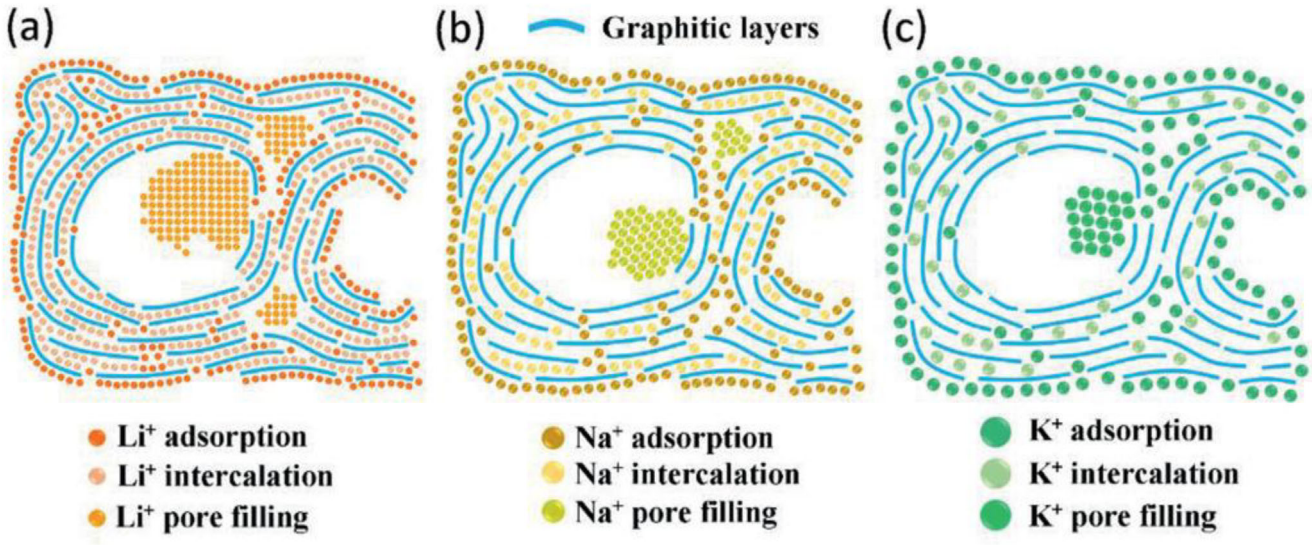

Figure 4. The electrochemical storage routes in WHC of a) Li+ ions, b) Na+ ions, and c) K+ ions. Reproduced with permission.[59] Copyright 2021, Wiley.

3.1.1. Li-Storage Chemistry

The primary storage mechanism of Li+ ions in WHC remains a subject of ongoing debate. Based on the recent reviews, the following mechanisms are proposed for the Li accommodation in WHC: i) Li^+ intercalation, ii) surface chemisorption-bulk chemisorption, iii) adsorption-intercalation, and iv) adsorption-intercalation and Li plating,[58,59,61] which can be summarized as follows:

- Li^+ intercalation: The intercalated Li^+ ions are stored in either closed-pore structures (possessing smaller diameters less than <6 Å) or the graphitic lattice domains.
- Surface chemisorption-bulk chemisorption: The diffusion of surface chemisorbed Li^+ ions into inner WHC structures by the concentration gradient. After that, the bulk chemisorption is induced on the pore surface with a diameter larger than the critical size (e.g., greater than 6 Å). The intercalation takes place when the pore surface has a smaller diameter.
- Adsorption-intercalation: The interaction occurs between Li^+ ions and the graphene layers, whereas the adsorption appears on the surface/defects.
- Adsorption-intercalation and Li plating: The accommodation of Li+ ions intercalated in the pseudo graphitic areas, leading to the formation of Li plating as the film under the solid electrolyte interphase (SEI) layer. Then, the dendrites are formed during the reactions in Li plating.

3.1.2. Na-Storage Chemistry

There are two voltage slope regions, which result in four distinct categories of the proposed Na^+ insertion/extraction, namely, intercalation filling, adsorption intercalation, adsorption filling, and adsorption intercalation filling (**Figure 5**).[52,53,58,61] The key concepts are summarized briefly as follows:

- Intercalation filling: Initially, the insertion of Na+ ions among the graphite layers occurs in the high-voltage (>0.1 V) slope region. Consequently, in the low voltage (≈0–0.1 V) plateau region, the ion adsorption filled in the carbon microspores is formed by chaotic stacking of pseudographitic domains.
- Adsorption intercalation: The adsorption of Na^+ ions occurs first on the defect sites of the carbon surface in the slope region. Then, these ions are inserted into the graphitic planes in the plateau region.
- Adsorption filling: The Na^+ ions are sodiated into the edge of carbon layers and nanovoids of hard carbon anodes. This mechanism is associated with the fast charging of SIBs using hard carbon anodes.
- Adsorption intercalation filling: In the slope capacity (>0.2 V) area, the Na^+ ions are adsorbed at the edges of chaotic stacked pseudographitic planes and defect locations in carbon structures. Meanwhile, the plateau capacity is divided into two regions. The Na^+ ions intercalated into pseudographitic planes occur in the first region (≈0.2–0.05 V), whereas these ions fill in the closed-pore structures in the second one (<0.05 V).

3.2. Rechargeable Batteries

The hard carbons obtained after carbonization show a more porous structure compared to the original waste feedstock. Nevertheless, their structural features do not align with the requirements of electrodes for EES devices, which essentially require further porous structures and larger surface areas. Hence, the DC is usually conducted after the HTC. The literature review is based on the comparison between one-step DC and two-step HTC-DC, as shown in **Figure 6**.

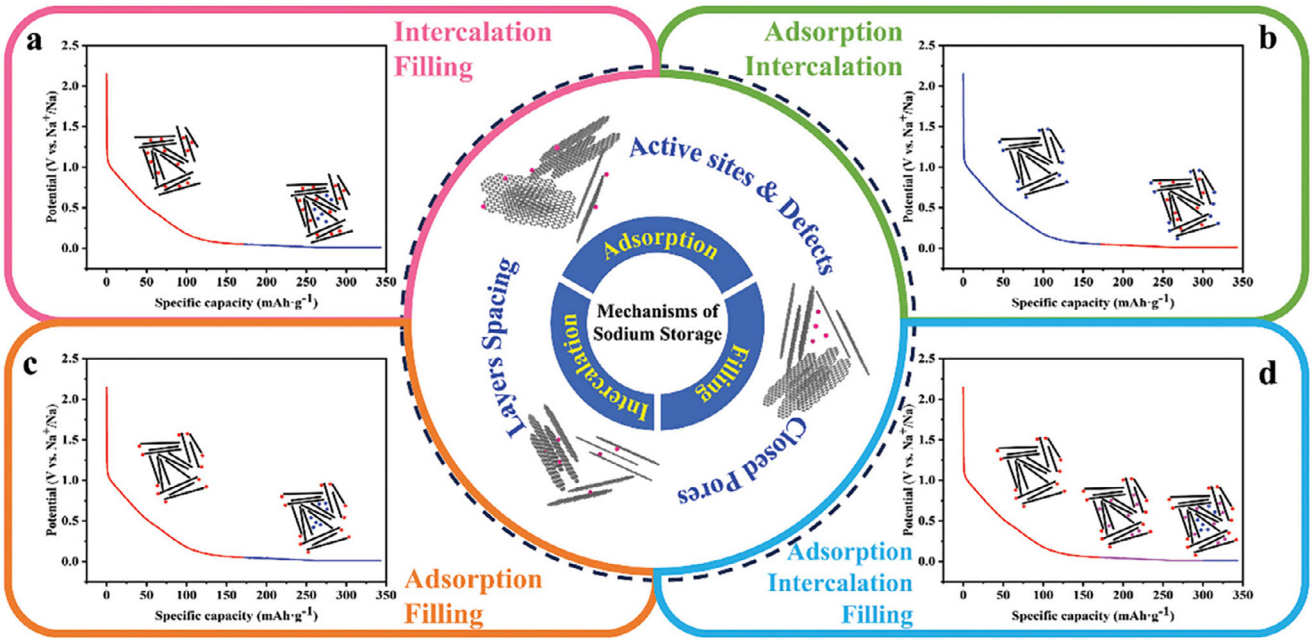

Figure 5. A summary of four different categories of Na^+ ion storage mechanisms in waste-derived hard carbon. Reproduced with permission.[53] Copyright 2025, Wiley.

3.2.1. Lithium-Ion Batteries

The commercial LIB configurations have many layers, as illustrated in **Figure 7a**.[62] Among them, the anode plays a critical role in determining the price and capacity (such as energy density) of a cell.[62] As shown in Figure 7b, anode materials include graphite, non-graphitizable carbon, and graphitizable carbon. Graphite has been widely fabricated as an anode in commercial LIBs for electric vehicles and portable electronic devices. In general, graphite production involves heating petroleum coke at extremely high temperatures (>2000 °C) for a prolonged residence time, which requires high energy consumption. This results in a costly synthesis process, while also contributing to a large carbon footprint and posing a significant environmental threat.[14,63–65] Therefore, apart from recycling spent graphite from end-of-life LIBs,[46] replacing traditional synthetic graphite with non-graphitizable- and graphitizable carbon materials based on non-fossil resources, such as WHC from waste, is emerging as an eco-friendly methodology. HTC has played a critical role in the production of graphitic WHC anodes for LIBs.[66] WHC-derived anodes for LIBs from previous attempts are tabulated in **Table 2**. There has been very little research into the comparison between HTC-DC and DC with the aim of WHC electrodes of LIBs.

The abundant waste of hazelnut shells has been studied for various renewable applications, such as WHC-based anode materials for LIBs via the HTC process.[67,68] Compared to the absent HTC-based WHC, the one produced with HTC exhibits a smaller O/C ratio, as well as a larger surface area and graphitization structure, which is beneficial for lithium battery performance.[68] Another well-known waste is rice husk, which is abundantly available in rice-producing countries (e.g., Vietnam, China, India).

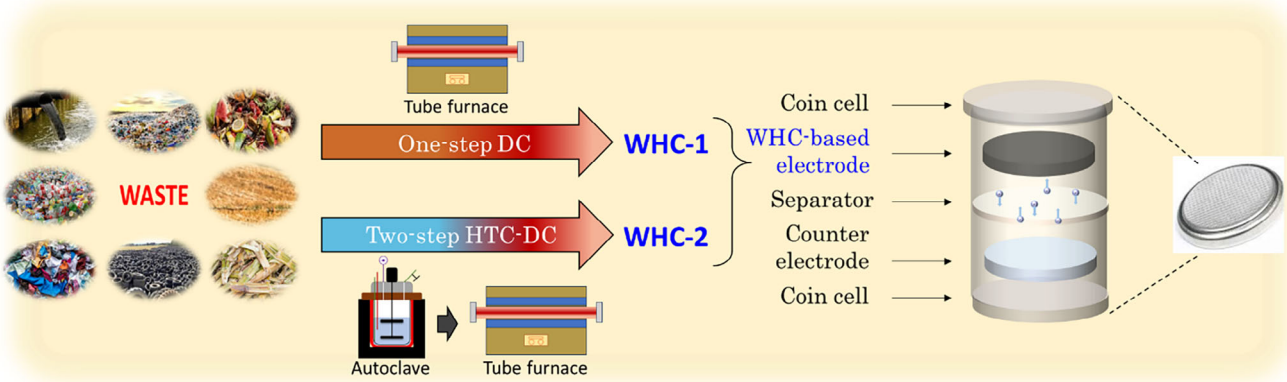

Figure 6. Schematic diagram of the comparison between DC and HTC-DC methods.

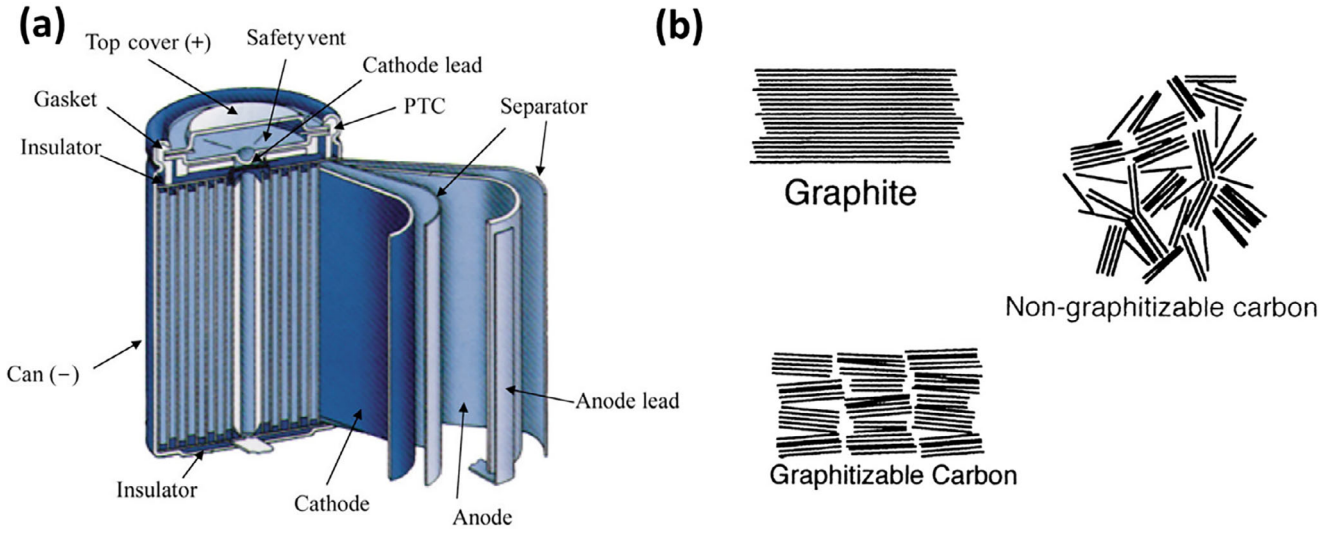

Figure 7. a) A configuration of lithium-ion batteries; b) Structure of carbon-based anodes for LIBs. Reproduced with permission.[62] Copyright 2025, Wiley.

Thanks to its high silica content, this important by-product has been widely used as an anode for LIBs.[73] Wang et al. produced carbon-silica electrodes through DC[70] and the combination of HTC and DC.[31] The author investigated that the formation of fibrous-like mesoporous carbon by the conversion of the remaining cellulose through HTC may be attributed to the greater capacity (396 mAh g^{-1}) of the anode produced through the HTC-DC process[31] compared to that of non-HTC-produced anodes (325 mAh g^{-1}) (see **Figure 8**).[70]

Uniform lignin-based carbon microspheres were formed using the HTC-DC.[71] As an anode in a lithium half-cell configuration, its reversible capacity was 180.6 mA g^{-1} with an ICE of 52.8%. After a 100-cycle cycling stability test, the device retained 98% of the initial capacity. When the carbonization increased, the electrochemical performance reduced. The author claimed that the reduced interlayer distance was observed at higher carbonization operating temperatures, impeding the insertion of Li ions and, as a result, the discharge capacity was adversely affected. In another effort, the as-synthesized corn straw-derived anodes formed unique spherical and cross-linked structures due to the hydrothermal conditions, resulting in a capacity of 577 mAh g^{-1} in Li devices.[72]

Table 2. A summary of half-cell LIBs performance using HC-based electrodes.

Feedstock	Carbonized operating condition			Half-cell performance					Refs.
	HTC (reactor type, solvent)	HTC (temp., time)	DC (temp., time)	Electrolyte	Current density [mA g^{-1}]	Specific capacity [mAh g^{-1}]	ICE [%]	Capacity Retention [%, cycles]	
Hazelnut shells	SSA citric acid solution	250 °C 7.5 h	600 °C 2 h	1 M $LiPF_6$ (EC:DMC)	372	723.66	45.64	40%, 100 cycles	[67]
Hazelnut shells	SSA citric acid solution	220 °C 12 h	900 °C 2 h	1 M $LiPF_6$ (EC:DMC)	10	530	44	42%, 20 cycles	[68]
Hazelnut shells	SSA citric acid solution	220 °C 12 h	900 °C 2 h	1 M $LiPF_6$ (EC:DMC)	10	1108	56	52%, 20 cycles	[68]
Glucose	0.1-L SSA Water	230 °C 12 h	1000 °C 2 h	1 M $LiPF_6$ (EC:DMC)	30	350	-	-	[69]
Rice husk	0.025 LTeflon-lined SSA Water	230 °C 24 h	900 °C 4 h	1 M $LiPF_6$ (EC:DMC)	75	396	52	-	[31]
Rice husk	-	-	900 °C 4 h	1 M $LiPF_6$ (EC:DMC)	74	325	53	-	[70]
Lignin	Teflon-lined SSA, HCl solution	230 °C 24 h	900 °C 3 h	1 M $LiPF_6$ (EC:DEC)	20	180.6	52.8	98%, 100 cycles	[71]
Corn straw	SSA, water	230 °C 36 h	600 °C -	1 M $LiPF_6$ (EC:DMC)	74.4	577	51	-	[72]

Abbreviations: ICE, Initial Coulombic Efficiency; SSA, Stainless Steel Autoclave; $LiPF_6$, Lithium hexafluorophosphate; EC, ethylene carbonate; DMC, dimethyl carbonate; DEC, diethyl carbonate.

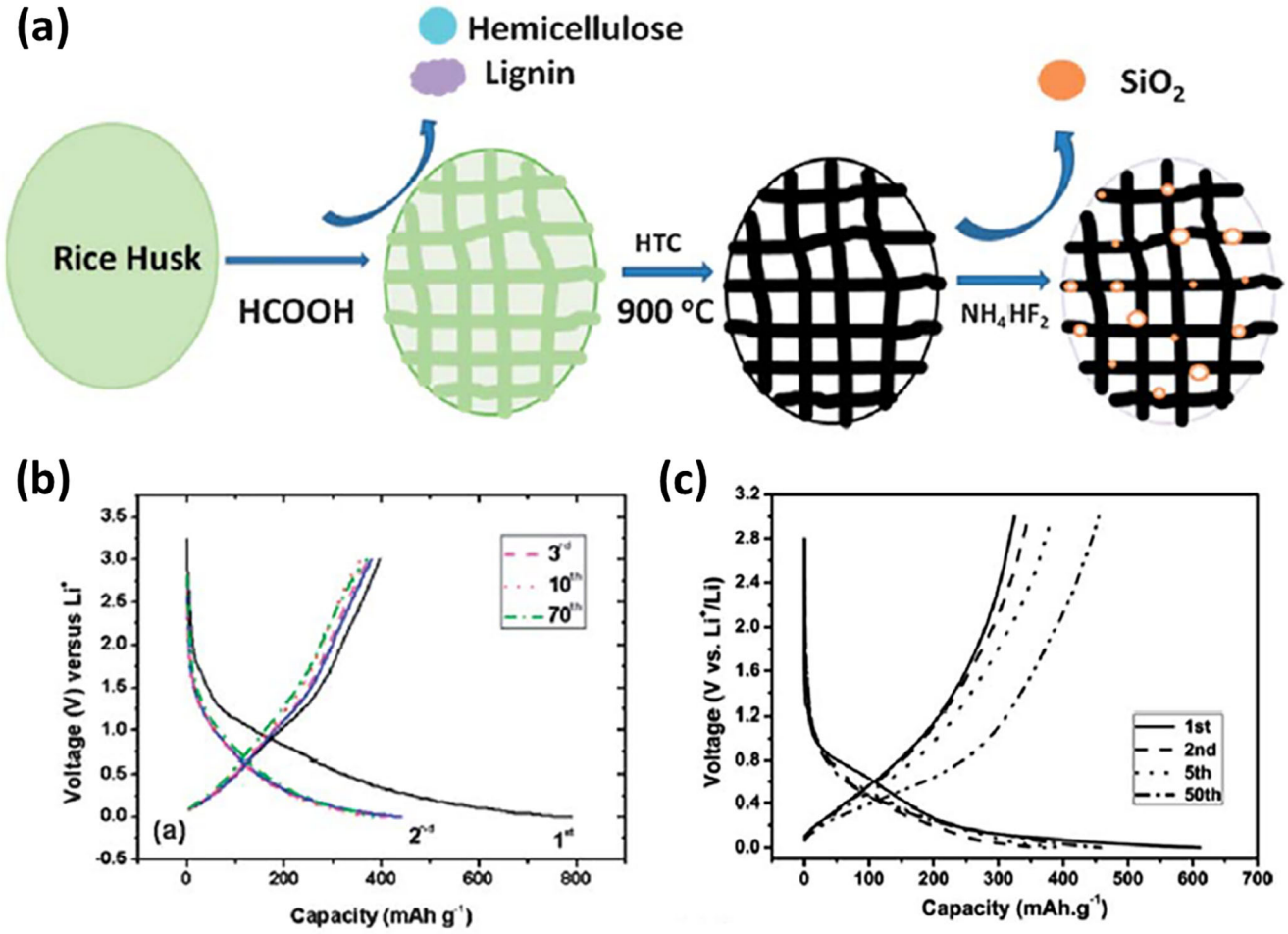

Figure 8. a) Scheme for the production of rice husk-derived WHC and the lithium electrochemical performance of b) as-synthetic anode with HTC at a current density of 75 mA g^{-1}. Reproduced with permission.[31] Copyright 2013, Royal Society of Chemistry. c) The lithium electrochemical performance of the as-prepared anode without HTC at a current density of 74 mA g^{-1}. Reproduced with permission.[70] Copyright 2014, Royal Society of Chemistry.

3.2.2. Sodium-Ion Batteries

Recent efforts on SIBs have been increasingly driven by the significantly cheaper and higher abundance of sodium (Na) in the Earth's crust compared to lithium (2.3% vs 0.0017%), making it one of the most promising alternatives for future large-scale energy storage systems. Primarily, the electrochemical performance of SIBs (e.g., storage capacity, cycling stability, and energy density) heavily depends on the anode materials.[74] Among all current anodes, due to its short-range microcrystalline graphite structure, hard carbon has drawn considerable attention for its facile synthesis, cost-effectiveness, and excellent electrochemical performance (e.g., low average potential, improved ICE, and high reversible capacity). It is also the primary choice for the anode in commercial SIBs.[74] Importantly, these hard carbon anodes can be synthesized from a wide range of waste feedstock (e.g., agriculture, biomass), leading to low cost and being environmentally benign for SIBs.[7,75] **Table 3** presents a list of previous attempts related to the two-step WHC procedure, such as HTC followed by the DC step. Compared to LIBs, there are more studies on the WHC for SIBs. This is because i) the emergent bumping of low-cost SIBs, ii) the compatibility of WHC's properties (e.g., porous structure allowing Na ions' storage) as anodes for SIBs. Meanwhile, graphite anode has been developed and commercialized for LIBs. Additionally, numerous investigations have been conducted on upcycling spent graphite for LIBs.[14,76,77]

Three different types of biomass waste (e.g., spent coffee grounds (COFF), sunflower seed shells (SEED), and rose stems (STEM)) were tested with and without HTC pretreatment.[29] Compared to other as-prepared samples, WHC-derived SEED electrodes in half-cell configuration provided excellent ICE improvement, specific discharge capacity, and high-capacity retention after 1000 cycles. The presence of HTC, followed by DC, in the SEED sample led to the formation of C = O/COOH groups in the WHC, resulting in higher C yields and enhancing the incorporation of O and N. They also exhibited expanded graphitic interlayer space. These features can be attributed to higher ICE and rate capability than as-prepared electrodes without HTC,[29] which is in agreement with other studies.[69,82]

To gain insight into the role of HTC in producing WHC for sustainable EES, glucose was used as the carbon source for hard carbon produced by HTC-DC, which was employed in

Table 3. A summary of half-cell SIBs performance using WHC-based electrodes.

Feedstock	Operating condition			Half-cell performance					Refs.
	HTC (reactor type, solvent)	HTC (temp., time)	DC (temp., time)	Electrolyte	Current density [mA g^{-1}]	Specific capacity [mAh g]$^{-1}$	ICE [%]	Capacity Retention (%, cycles)	
Spent coffee ground	SSA	250 °C 24 h	1200 °C 2 h	1 M $NaPF_6$ (EC:DMC)	24.8	210	30	78.46%, 500 cycles	[29]
	-	-	1200 °C 2 h		24.8	200	34	-	
Sunflower seed shells	SSA	250 °C 24 h	1200 °C 2 h		24.8	290	76	86.05%, 500 cycles	[29]
	-	-	1200 °C 2 h		24.8	190	50	-	
Rose stems	SSA	250 °C 24 h	1200 °C 2 h		24.8	240	50	84.95%, 500 cycles	[29]
	-	-	1200 °C 2 h		24.8	180	40	-	
Corn cob	0.3-L SSA	250 °C 24 h	1200 °C 2 h	1 M $NaPF_6$ (EC:DMC)	24.8	268.54	73.49	-	[78]
	-	-	1200 °C 2 h		24.8	265.17	43.39	-	
Grape seed	0.3-L autoclave	250 °C 24 h	1200 °C 2 h		24.8	244.94	60.25	-	[78]
Grape seed	-	-	1200 °C 2 h		24.8	158.42	66.47	-	
River driftwood	2 L high-pressure reactor	200 °C 12 h	1400 °C 1 h	1 M $NaPF_6$ (EC:DMC:FEC)	37.2	300	83	98%, 100 cycles	[47]
Switchgrass	0.6-L SSR DI H_2O	220 °C 12 h	1600 °C 2 h	1 M NaOTf (DGM)	100	313.4	84.8	98.4%, 100 cycles	[24]
	-	-	1600 °C 2 h		100	235.5	75.91	31%, 100 cycles	
Shaddock peel	0.12-L Teflon-lined SSA, H_2SO_4	180 °C 24 h	600 °C 3 h	1 M $NaClO_4$ (EC:DEC)	50	287.3	57	93.8%, 500 cycles	[79]
Sucrose	SSA	190 °C	1600 °C 2 h		30	220	83	93%, 100 cycles	[80]
Glucose	SS jacket	200 °C 2 h	1300 °C 2 h	1 M $NaClO_4$ (EC:DMC)	30	347.4	85	73.1%, 300 cycles	[7]
	Carbolite STF furnace	-	1300 °C 2 h		30	261.3	85	0%, 300 cycles	[7]
Glucose	0.2-L autoclave reactor vessel	200 °C 12 h	1500 °C 2 h	1 M $NaPF_6$ (EC:DMC)	30	293	85	-	[81]
Glucose	-	230 °C 12 h	1500 °C 2 h	1 M $NaPF_6$ (EC:DMC)	30	340	86.9	-	[69]
Corn stalk powder	0.1-L PTFE-lined autoclave	160 °C 24 h	1000 °C 1 h	1 M NaOTf (DGM)	60	270	60	97%, 100 cycles	[82]
	-	-	1000 °C 1 h		60	233.4	58.4	97%, 100 cycles	[82]
Vine shoots	0.1-L PTFE-lined SSA, water	180 °C 12 h	1000 °C 2 h	1 M NaTFSI (EC:DMC)	100	236	79.4	77%, 250 cycles	[32]
	0.1-L PTFE-lined SSA, pig manure	180 °C 12 h	1000 °C 2 h	1 M NaTFSI (EC:DMC)	100	205	72	92%, 250 cycles	
	0.1-L PTFE-lined SSA, pig manure	180 °C 12 h	1000 °C 2 h HCl	1 M NaTFSI (EC:DMC)	100	237	71	81%, 250 cycles	

(*Continued*)

Table 3. (Continued)

Feedstock	Operating condition			Half-cell performance					Refs.
	HTC (reactor type, solvent)	HTC (temp., time)	DC (temp., time)	Electrolyte	Current density [mA g^{-1}]	Specific capacity [mAh $g]^{-1}$	ICE [%]	Capacity Retention (%, cycles)	
0.1-L PTFE-lined SSA, pig manure	180 °C 12 h with manure	1000 °C 2 h HCl	1 M $NaPF_6$ (DGM)	100	252	73	88%, 250 cycles		
Vine shoots	0.1-L Teflon-lined SSA, water	180 °C 12 h	1000 °C 2 h	1 M NaTFSI (EC:DMC)	100	246	71	-	[83]
	0.1-L Teflon-lined SSA, water	180 °C 12 h	1000 °C 2 h	1 M $NaPF_6$ (DGM)	100	215	69	90%, 250 cycles	
	0.1-L Teflon-lined SSA, HCl	180 °C 12 h	1000 °C 2 h	1 M $NaPF_6$ (DGM)	100	283	77	86%, 250 cycles	
	0.1-L Teflon-lined SSA, H_3PO_4	180 °C 12 h	1000 °C 2 h	1 M $NaPF_6$ (DGM)	100	281	68	87%, 250 cycles	
Reed straw	-	200 °C 24 h	1300 °C 3 h	1 M $NaClO_4$ (EC:DEC)	25	372	77.03	84%, 200 cycles	[84]
	-	200 °C 24 h	1100 °C 3 h	1 M $NaClO_4$ (EC:DEC)	25	260	73	87%, 200 cycles	
Carbon dot-based supernatant waste	0.05-L Teflon-lined SSA, water	200 °C 12 h	1300 °C 1 h	1 M $NaClO_4$ (EC:DMC)	30	302	91	96%, 100 cycles	[85]
Carbon dot-based solid	0.05-L Teflon-lined SSA, water	200 °C 12 h	1300 °C 1 h		30	178	75	82%, 100 cycles	
Almond shells	0.15-L Teflon-lined SSA, water	180 °C 24 h	1100 °C 5 h	1 M $NaPF_6$ (DGM)	37.2	317.1	85.9	91%, 600 cycles	[86]
	0.15-L Teflon-lined SSA, H_2SO_4	180 °C 24 h	1100 °C 5 h		37.2	290.1	80.1	90.6%, 600 cycles	
	-	-	1100 °C 5 h		37.2	263.4	80.0	80.7%, 600 cycles	

Abbreviations: SSA, stainless steel autoclave; SSR, stainless steel reactor; FC, full cell; ICE, Initial Coulombic Efficiency; Glucose, D-(+)-glucose, ≥99.5%, Sigma-Aldrich; NaOTf, Sodium trifluoromethanesulfonate; NaTFSI, Sodium trifluoromethanesulfonimide; $NaClO_4$, sodium percloride; $NaPF_6$, Sodium hexafluorophosphate; DMG, Diethylene glycol dimethyl ether; DMC, dimethyl carbonate; EC, ethylene carbonate; DEC, diethyl carbonate.

different battery technologies.[69] For example, while WHC was fabricated as anodes, the resulting reversible capacity based on lithium-, sodium-, and potassium-ion half cells (KIBs) achieved 350, 340, and 250 mAh g^{-1}, respectively. The ICEs of WHC in LIB, SIBs, and KIBs were 51.3%, 86.9%, and 60.3%, respectively. For further investigation, the electrochemical performance of full cells with commercial cathodes such as $LiNi_{0.8}Co_{0.1}Mn_{0.1}O_2$ (NCM811) for LIBs, $Na_3V_2(PO_4)_3$ (NVP) for SIBs, and perylene-3,4,9,10-tetracarboxylic dianhydride (PTCDA) for KIBs was conducted. The Li-, Na-, and K-ion full cells delivered excellent capacities of 380 mAh g^{-1} at 30 mA g^{-1}, 329 mAh g^{-1} at 30 mA g^{-1}, and 207.9 mAh g^{-1} at 25 mA g^{-1}, respectively. Titirici et al., found that the HTC plays a vital role as a pretreatment step for HC preparation before the DC step. Also, HTC results in enhanced electrochemical performance, greater carbon yields, and reduced carbon emissions.[7,69,81] Intriguingly, another study exhibited that the Global Warming Potentials (GWPs) generated for WHC anodes (HG1300) by the electricity of the HTC (0.52 kg $CO_{2eq/kg}$) and subsequent DC (0.30 kg $CO_{2eq/kg}$) was also lower than that of anodes (DG1300) via one-step DC (1.08 kg $CO_{2eq/kg}$), demonstrating the lower energy consumption and carbon emissions of the two-step process.[7] For the electrochemical assessment in a sodium half-cell configuration (**Figure 9**), the resulting reversible capacities of HG1300 and DG1300 were estimated to be 347.4 and 261.3 mAh g^{-1}, respectively, at a current density of 0.1 C. Meanwhile, the cycling stability testing showed that the HG1300 cell retained 73.1% of its initial capacity, whereas the DG1300 cell failed after 300 cycles.

Diverse agro-industrial biowaste was converted into HC using one and two carbonization steps and tested in SIBs technology. Alexander et al., converted corncob, apple pomace, olive mill solid waste, defatted grape seed, and dried grape skin into HC using both DC and HTC pathways.[78] The resultant half-cell configuration showed that the discharge capacity and ICE of corncob-derived anodes using HTC-DC were estimated to be 268.54 mAh g^{-1} and 73.49%, respectively. Meanwhile, the ICE was reduced to 46.39% in the DC case, demonstrating the positive effect of HTC. In another trial, spent coffee grounds, sunflower seed shells, and rose stems were converted into carbon anodes through DC and HTC-DC. Their electrochemical

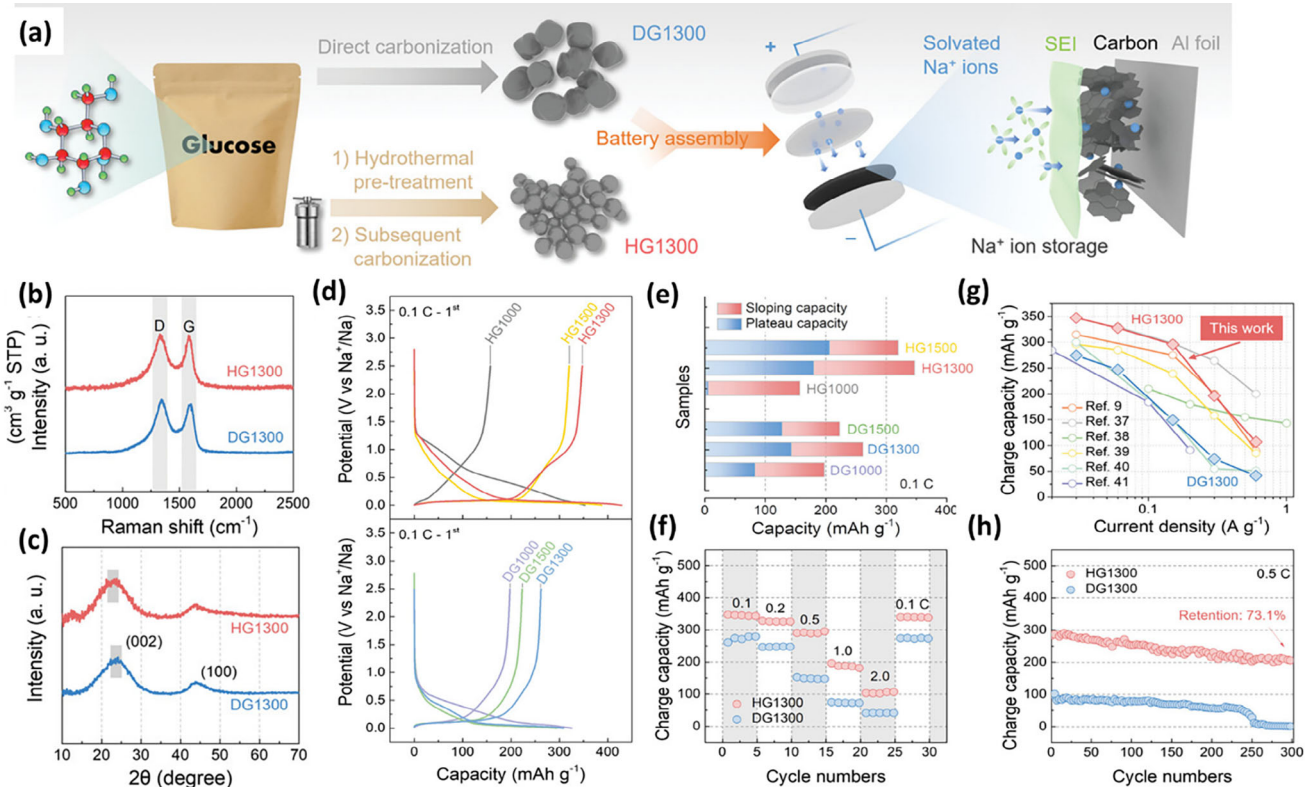

Figure 9. a) An overview production of glucose-based hard carbons through two different routes: i) direct carbonization at 1300 °C (namely DG1300) and ii) coupling HTC (at 200 °C) with direct carbonization at 1300 °C (namely HG1300); b) Raman spectra and c) XRD of two produced DG1300 and HG1300; d–h) Electrochemical performance of DG and HG electrodes: d) The GCD curves of various samples at 0.1 C (1 C = 300 mA g^{-1}); e) The sloping and plateau capacities of hard carbon electrodes, f) Rate performance from 0.1 to 2.0 C of DG1300 and HG1300, g) A comparison related to charge capacities of DG1300 and HG1300 with previous studies, h) Cycling stability recorded at 0.5 C. Reproduced under the terms of the CC-BY-4 license.[7] Copyright 2022, Elsevier.

behavior was further assessed in sodium half-cells. Based on the galvanostatic charge-discharge (GCD) curves, the reversible discharge capacity of sunflower seed shells-based anode synthesized via the HTC-DC processes was found to be 290 mAh g^{-1}, which was higher than that of the produced anode using only DC step (190 mAh g^{-1}). The result provided valuable insights into effectively utilizing HTC-DC for sustainable SIBs from abundant biowaste resources. In another study, the produced WHC derived from river driftwood using HTC-DC was employed for the SIB anode. The maximum reversible capacity and ICE reached 300 mAh g^{-1} and 83%, respectively.[47] Another interesting WHC is reed straw. Its resultant data showed an impressively high reversible capacity of 372.0 mAh g^{-1} with excellent ICE of 77.03%.[84]

Recently, an investigation into switchgrass-derived hard carbon anodes for SIBs demonstrated that HTC played an effective role in increasing the ICE and reversible specific capacity (see **Figure 10**).[24] After two-step HTC-DC processes, the half-cell electrochemical performance achieved a high reversible capacity of 313.4 mAh g^{-1} with a promising ICE of 84.8% and exceptional cycling stability (retained 98.4% of initial capacity after 100 cycles). Meanwhile, the resultant device produced a hard carbon-based anode without the HTC step, revealing a significantly lower capacity (235.5 mAh g^{-1}), ICE (75.91%), and cycling stability (31% after 100 cycles). The authors discovered that the main reason is that the presence of the HTC step efficiently eliminates impurities and hemicellulose in switchgrass waste, thereby reducing the surface area and improving the prestabilization of the as-prepared hard carbon before the DC step. This limits the SEI formation, resulting in outstanding device performance. The full cell was fabricated and delivered a specific capacity of 99 mAh g^{-1} with a capacity retention of 78% after 100 cycles.

The usually ignored carbon-based waste in the supernatant of HTC was also a promising anode for SIBs.[85] In this study, both carbon in the liquid and solid phases, after separation in the HTC process, were carbonized at different temperatures to produce carbon-based anodes. In the half-cell configuration, the resultant device of carbon waste-based anode delivered a specific capacity of 302 mAh g^{-1} with the ICE of 91%, which was superior to those of the conventional solid HC anode (178 mAh g^{-1} and 75%, respectively) under identical conditions. The author found that more ordered structures, fewer defects, and a lower surface area of the carbon waste resulted in a significant improvement in capacity and ICE. The research also demonstrated that wet waste can be effectively converted into carbon materials using the HTC method.

Solvents have a significant effect on the HTC process, particularly in terms of WHC properties for SIBs applications. Recently, various WHCs with diverse surface areas and pore sizes from

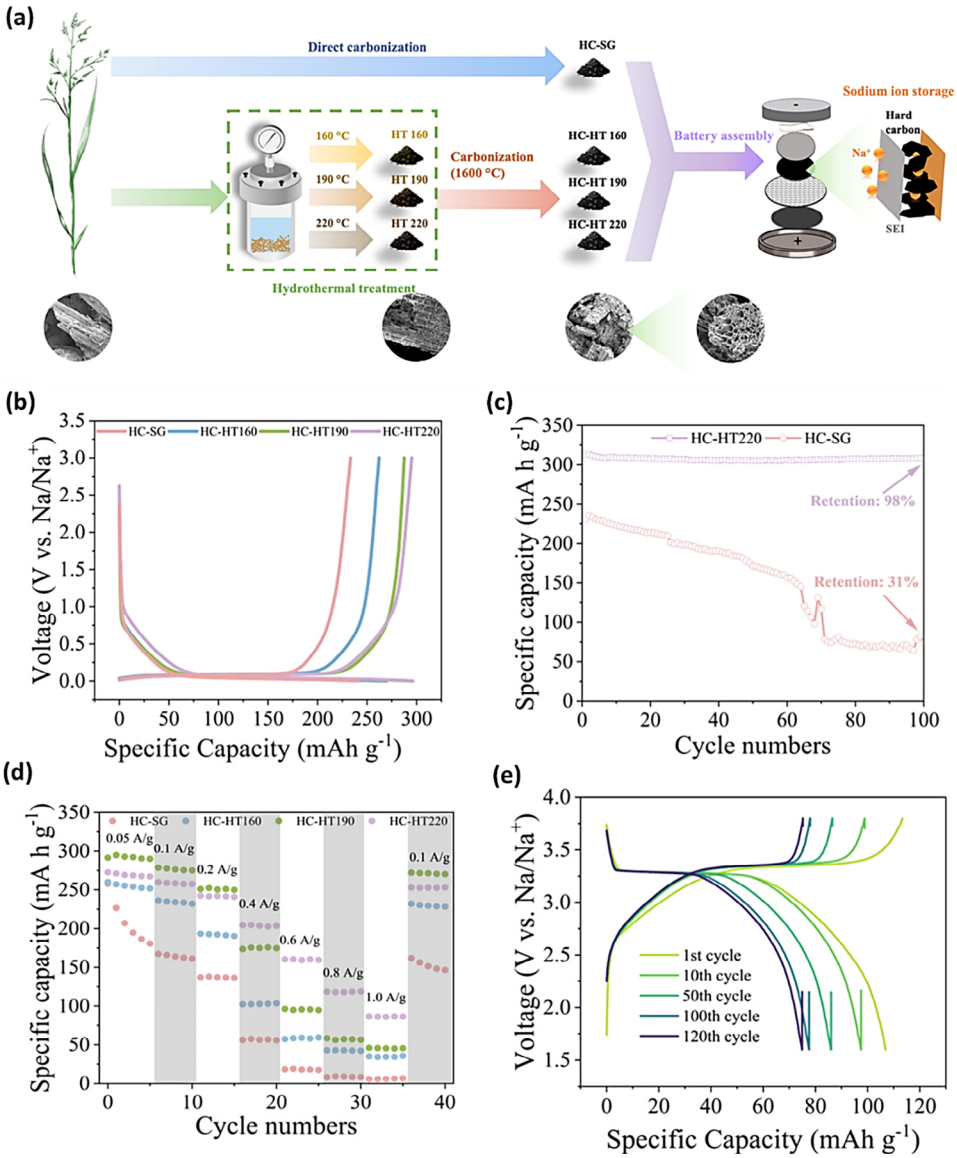

Figure 10. a) An overview scheme of the synthesis routes of switchgrass-derived hard carbons; b–e) Electrochemical performance: b) second cycle of galvanostatic charge/discharge (GCD) curves of HC-SG, HC-HT160, HC-HT190, and HC-HT220 at 0.1 A g^{-1} within the potential range of 0.001–3 V versus Na/Na^+; c) cycling performance at 0.1 A g^{-1}, of HC-SG and HC-HT220 after 100 charging–discharging cycles; d) rate performance of HC-SG, HC-HT160, HC-HT190, and HC-HT220 at the current densities of 0.05, 0.1, 0.2, 0.4, 0.6, 0.8, and 1.0 A g^{-1} for 5 cycles each; e) GCD curves of the pre-sodiated full-cell battery using the HC-HT220 anode at 0.1 A g^{-1} after 1, 10, 50, 100, and 120 cycles. Reproduced under the terms of the CC-BY-4.0 license.[24] Copyright 2024, American Chemical Society.

vine shoots were synthesized via HTC, followed by DC, using water, pig manure, and acid solutions (e.g., HNO_3, HCl, H_2SO_4, and H_3PO_4) as shown in **Figure 11a**.[32,83] After that, those WHC were employed as anodes for SIBs with two electrolytes (e.g., NaTFSI/EC: DMC and $NaPF_6$/DGM). Among them, the anodes derived from acid-catalyzed HTC using HCl and H_3PO_4 (namely HCl-1000 and H_3PO_4-1000) exhibited superior specific capacities of 280 mAh g^{-1}, accompanied by corresponding ICEs of 77% and 68%, respectively. The studies show that the acid-assisted HTC process not only provides a mixed structure of crystalline and amorphous nature for a high-performing WHC-based anode in SIBs but also promotes a sustainable EES and circular economy model.

Very recently, Chen et al. effectively demonstrated the role of HTC followed by DC to produce WHC-based anodes for SIBs from almond shell waste (HY).[86] The comparison of anode morphology and sodium storage behavior was conducted for samples synthesized using HTC with water and H_2SO_4 solvents (namely HC-W and HC-A, respectively), along with the standard sample (without HTC, namely HC-P). Intriguingly, under identical experimental conditions, the extraordinary reversible capacity of the HC-W anode achieved 317.1 mAh g^{-1} with the ICE of 85.9%.

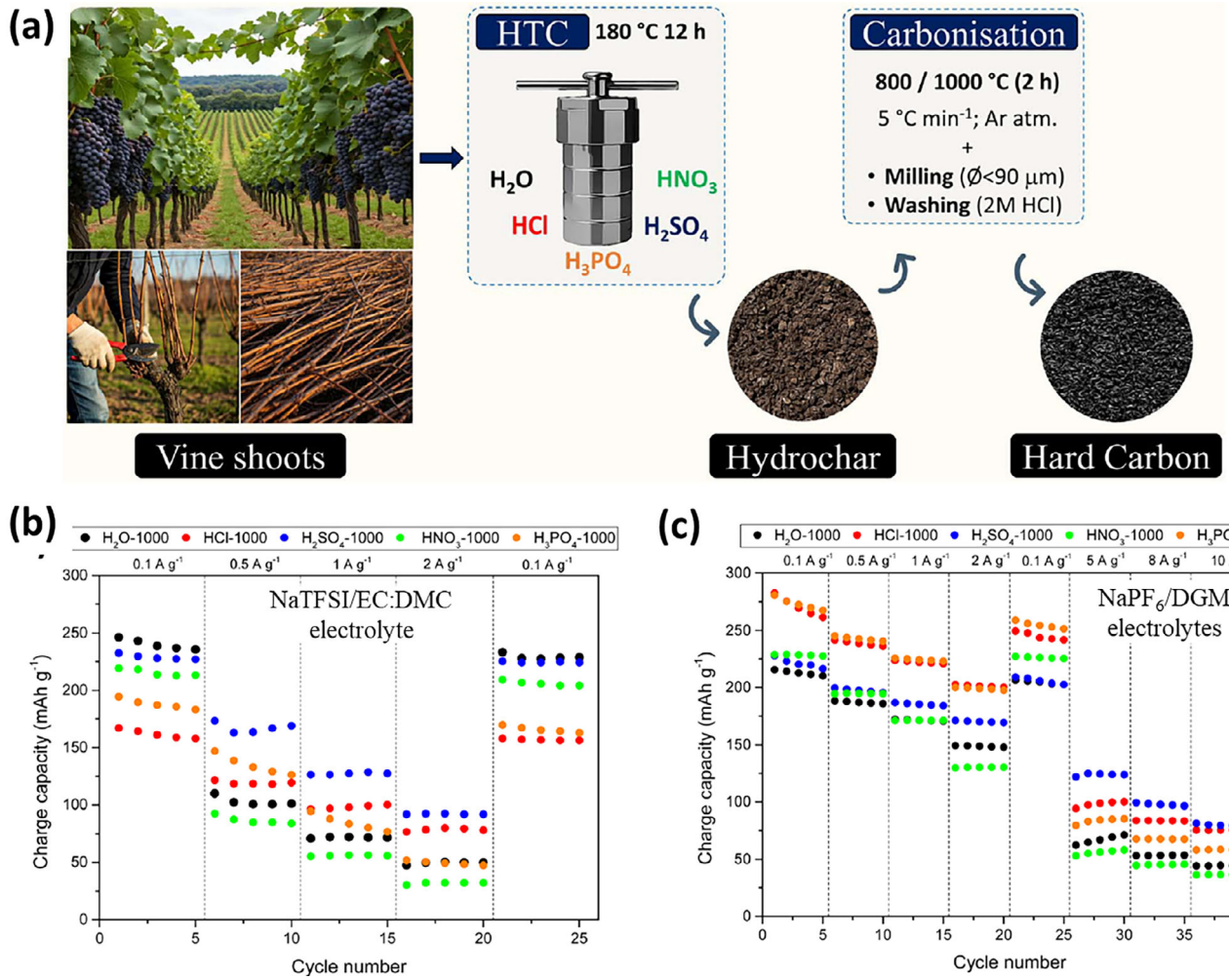

Figure 11. a) Scheme of the WHC preparation; b,c) Rate performance at various current densities in NaTFSI/EC:DMC and $NaPF_6$/DGM electrolytes, respectively. (H_2O-1000 (black), HCl-1000 (red), H_2SO_4-1000 (blue), HNO_3-1000 (green), and H_3PO_4-1000 (oragne)). Reproduced under the terms of the Creative Commons Attribution-Noncommercial 3.0 Unported license.[83] Copyright 2025, Royal Society of Chemistry.

In contrast, the lower electrochemical performance was observed for HC-A and HC-P (**Figure** 12h,k,l). According to ex and in situ analysis, the larger scale of graphitization under acidic HTL was not favorable for the electrochemical Na-ion storage. The durable structure with a small-scale graphitic structure of HC-W (under neutral HTL) during repeated sodium ion insertion and extraction is attributed to its excellent sodium-ion storage behavior.

3.3. Supercapacitors

In addition to battery technology, supercapacitors (SCs) play a crucial role by offering high specific power and relatively high specific energy.[87] Their compact size and lightweight design make them suitable as a power source for various electronic applications. For instance, SCs have successfully addressed the need for high power output during short-term acceleration and high capacity for temporary energy storage in hybrid electric vehicles.[88] In an SC configuration, activated carbon (AC) has been intensively utilized as electrodes, as it can be produced from biomass waste feedstock through economical and green two-step synthesis approaches, such as the HTC process and subsequent activation. The HTC enriches the carbon content and transforms wet biomass into valuable products such as hydrochar (or WHC), which is a promising precursor for AC electrodes.[89,90] In this regard, unique attributes of WHC include a low degree of condensation and a high density of oxygenated functional groups. These features can be customized to create AC with high surface areas as well as specific and desirable characteristics for SCs.[91] Additionally, the HTC step also lowers the production cost of these AC electrodes from natural sources. Notably, the AC electrodes, after activation from WHC, exhibited a high degree of graphitization, thereby improving the capacitive behavior of the supercapacitors.[92,93] **Table** 4 provides a summary related to the facile two-step AC synthesis, specifically HTC followed by an activation step.

A study investigated electrochemical supercapacitors using AC electrodes from non-HTC and HTC-treated *Eucommia ulmoides* Olive (EUO) wood.[94] Compared to non-HTC-treated electrodes under identical conditions, the presence of the HTC

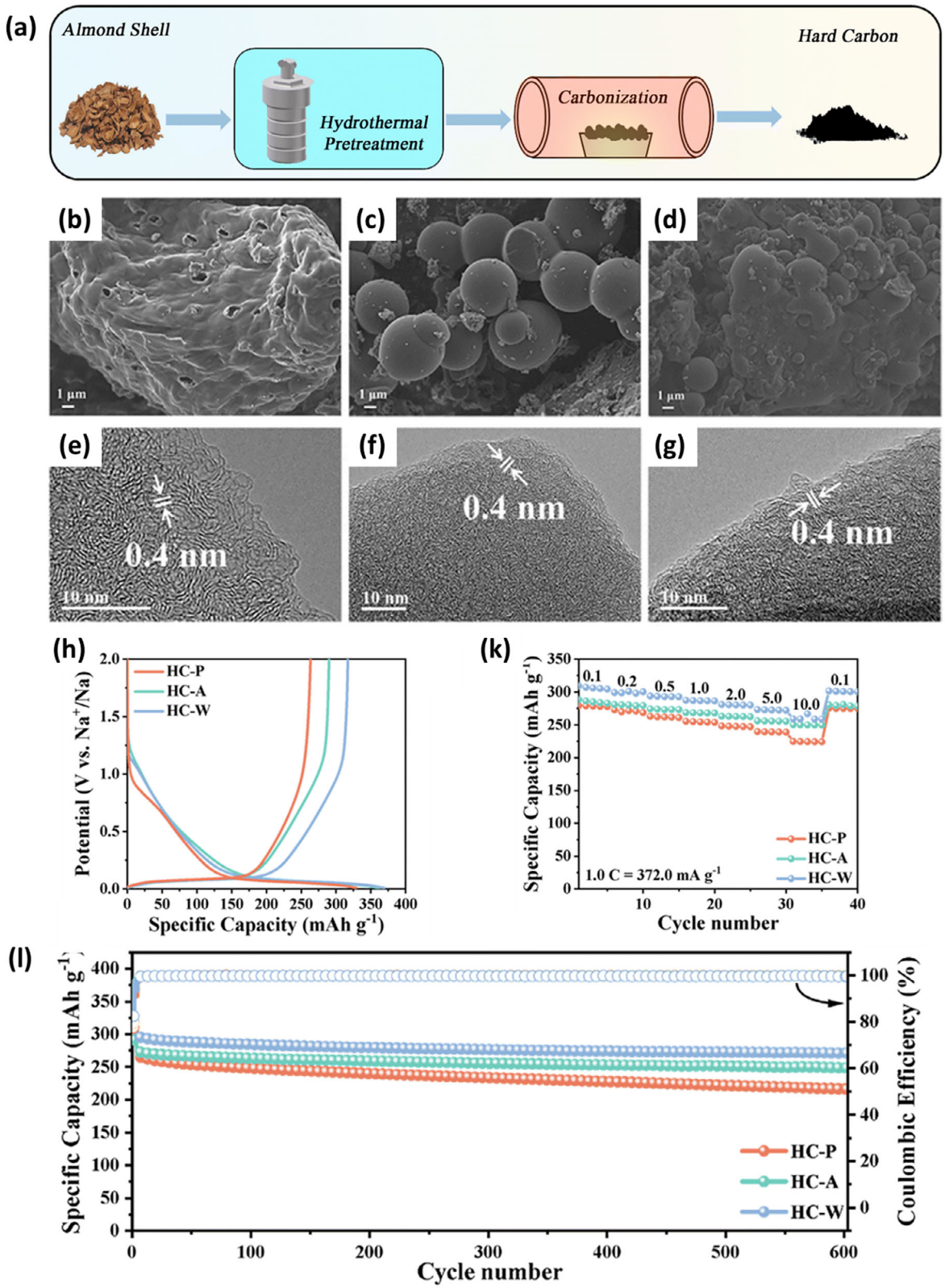

Figure 12. a) Preparing almond shell-derived HC through HTC and DC; b–d) SEM images of b) HC-P, c) HC-A, and d) HC-W; e–g) TEM images of e) HC-P, f) HC-A, and g) HC-W; h) The initial discharge/charge curves at 0.1C (1C = 372 mA g^{-1}); k) Rate performance; (l) Stability testing for 600 cycles at 1C of HC-P, HC-A, and HC-W; Reproduced under the terms of the Creative Commons Attribution 3.0 Unported Licence.[86] Copyright 2025, Royal Society of Chemistry.

Table 4. A summary of half-cell supercapacitor performance using WHC-based electrodes.

Feedstock	HTC (reactor type, solvent)	HTC (temp., time)	Activation (agent, temp., time)	Surface area [$m^2\ g^{-1}$]	Device configuration	Electrolyte	Specific capacitance [$F\ g^{-1}$]	Capacity retention [%, cycles]	Refs.
Oliver wood	1-L SS autoclave, water	170 °C 0.5 h	H_3PO_4, 550 °C 2 h	1456.69	three-electrode	1 M H_2SO_4	158 (at 0.2 A g^{-1})	95.3%, 1000 cycles	[94]
	-	-	H_3PO_4, 550 °C 2 h	1405.43	three-electrode	1 M H_2SO_4	158 (at 0.2 A g^{-1})	-	
Melon peels	0.1-L Teflon lined autoclave, water	330 °C 12 h	$ZnCl_2$, 800 °C 2 h	1459	symmetrical	PVDF gel polymer	161–170 (at 1 A g^{-1})	85%, 8000 cycles	[90]
	-	-	$ZnCl_2$, 800 °C 2 h	1238	symmetrical	PVDF gel polymer	135–148 (at 1 A g^{-1})	-	[90]
	-	-	EtOH, 20 days 800 °C 2 h	1381	symmetrical	PVDF gel polymer	153–158 (at 1 A g^{-1})	-	[90]
Peanut shell	0.05-L Teflon lined autoclave, H_2SO_4, water	170 °C 72 h	$ZnCl_2$, 800 °C 2 h	1393	symmetrical	PVDF gel polymer	168 (at 1.25 A g^{-1})		[95]
	-	-	EtOH, 30 days $ZnCl_2$, 800 °C 2 h	1537	symmetrical	PVDF gel polymer	189 (at 1.25 A g^{-1})		[95]
Soluble starch	0.1-L Teflon lined autoclave, water	180 °C 16 h	$KHCO_3$, 900 °C 2 h	1972.8	three-electrode	1 M H_2SO_4	369.8 (at 1 A g^{-1})	-	[96]
	0.1-L Teflon lined autoclave, water	180 °C 16 h	$KHCO_3$, 900 °C 2 h	1972.8	symmetrical	1 M H_2SO_4	60.2 (at 0.5 A g^{-1})	100.8%, 70 000 cycles	[96]
Jujun Grass	water	180 °C 10 h	KOH 900 °C 2 h	2838	three-electrode	6 M KOH	220 (at 1 A g^{-1})	-	[97]
	Ionic liquid	180 °C 10 h	KOH 900 °C 2 h	2532	three-electrode	6 M KOH	336 (at 1 A g^{-1})	-	[97]
Sunflower stalk	0.2-L polytetrafluoroethylene (PTFE) autoclave	230 °C 24 h	KOH 800 °C 2 h	1505	three-electrode	6 M KOH	365 (at 1 A g^{-1})	81%, 15 000 cycles	[98]
	0.2-L polytetrafluoroethylene (PTFE) autoclave	230 °C 24 h	KOH 800 °C 2 h	1505	symmetrical	6 M KOH	263 (at 0.5 A g^{-1})	95%, 15 000 cycles	[98]

(*Continued*)

Table 4. (Continued)

Feedstock	HTC (reactor type, solvent)	HTC (temp., time)	Activation (agent, temp., time)	Surface area [$m^2 g^{-1}$]	Device configuration	Electrolyte	Specific capacitance [F g^{-1}]	Capacity retention [%, cycles]	Refs.
Acacia gum	0.1-L Teflon lined autoclave, water	180 °C 12 h	KOH 800 °C 1 h	1832	three-electrode	6 M KOH	272 (at 1 A g^{-1})	93%, 1000 cycles	[99]
Bean curd stick	Teflon lined autoclave, water	200 °C 6 h	KOH 400 °C 1 h 700 °C 1 h	2609	three-electrode	6 M KOH	405 (at 0.5 A g^{-1})	90%, 10 000 cycles	[100]
Mixed waste (sewage sludge and coconut shell)	0.1-L Teflon lined autoclave, water	220 °C 3 h	KOH 700 °C 3 h	3003	symmetrical	6 M KOH	420 (at 0.5 A g^{-1})	94%, 10 000 cycles	[101]

process significantly enhanced the porosity and surface chemistry of WHC before the chemical activation. According to XRD and Raman characterization, the HTC-treated AC electrodes exhibited high graphitization during activation, resulting in superior capacitive behavior (158 F g^{-1}) and satisfactory long-term cycling stability. This also aligns with another recent report on various pretreatment methods developed using melon peel waste as starting precursors to produce ACs for gel-polymer electrolyte-based SCs.[90] Among these pretreated samples, the resultant devices using hydrothermally pre-treated AC electrodes exhibited the best capacitance (170 F g^{-1} at 1 A g^{-1}) and excellent stability (retained 85% of initial capacitance over 8000 cycles) due to the larger surface area and an appropriate amount of micro- and meso-porosity.

In another study, synthetic AC was made from low-cost soluble starch precursor and eco-friendly potassium bicarbonate ($KHCO_3$) as an activating agent for SCs and SIBs applications.[96] Since the AC possessed a high graphitic feature and a high surface area, the resulting SCs delivered a remarkable capacitance of 369.8 F g^{-1} at a current density of 1 A g^{-1}. Meanwhile, the sodium ion half-cell displayed a reversible capacity of 210.3 mAh g^{-1} at 0.05 A g^{-1} with extremely low ICE (≈25%). Jujun grass was used as a carbon source through HTC using water and ionic liquid solvents.[97] After activation, the highest specific capacitance in electrical double-layer capacitors was estimated to be 336 F g^{-1} at 1 A g^{-1} for ionic liquid-based carbon, due to its large accessible mesopores and a moderate proportion of micropores compared to carbon electrodes prepared using carbon because they possess large accessible mesopores and a moderate proportion of micropores in comparison to carbon electrodes prepared by water as a solvent.

4. Challenges and Future Perspectives

Despite these promising developments, most studies remain confined to laboratory-scale demonstrations. The diversity of feedstocks, processing routes, and device configurations makes it difficult to establish universal performance benchmarks. Moreover, the lack of standardized protocols for material characterization and electrochemical testing hinders cross-comparison and reproducibility. However, our analysis indicates that before WHC-based electrodes can be reliably realized at scale in LIBs, SIBs, and SCs devices, several significant challenges must be addressed.[102] This section discusses those critical bottlenecks and proposes prospective directions.

4.1. Challenges to Address

4.1.1. Feedstock Variability and Product Consistency

Biomass wastes are naturally diverse in moisture content, mineral/ash composition, and organic fractions (e.g., cellulose, lignin, extractives). This diversity results in different reaction pathways during HTC, producing hydrochars with varied morphologies, porosities, heteroatom contents, and electrochemical properties.[103] Additionally, many HTC studies use different operational protocols (e.g., temperature, pressure, residence

time, biomass loading), which worsens discrepancies in results. To facilitate meaningful comparison and reproducibility, the community should establish standard benchmarks for feedstock pre-characterization (proximate/ultimate analysis, ash speciation) and standardized HTC protocols (e.g., reference temperature/time sets). Moreover, advanced characterization techniques (e.g., Raman spectroscopy, XPS, synchrotron XRD, N_2 adsorption, electron microscopy) should be routinely used to link structural features (like degree of graphitization, defect density, pore interconnectivity) with electrochemical performance (including capacity retention and rate capability).

4.1.2. Scalability and Logistical Constraints

While HTC has been demonstrated in laboratory and pilot settings, industrial deployment remains limited. Significant challenges include the dispersed and low-density distribution of biomass sources, the high capital costs for pressurized reactors, and the logistical expenses involved in collection, transportation, and pre-treatment.[104] A thorough systems analysis is essential. Decentralized "mini-HTC" units near biomass sources, modular mobile reactors, or co-location with biomass processing facilities (e.g., pulp mills, municipal waste plants) could reduce transportation burdens. Collaborative, cross-sector partnerships among academia, industry, and government will be vital to developing feasible business models, support mechanisms, and economies of scale.

4.1.3. Reactor Engineering and Process Integration

Most existing HTC systems operate as batch reactors, which restrict throughput, scalability, and process control. To transition to industrial operation, continuous-flow or semi-continuous HTC designs with in situ monitoring, including temperature, pressure, solids concentration, and advanced control, are necessary. Additionally, integrating HTC with downstream or parallel processes, such as anaerobic digestion, solar-thermal heating, wastewater treatment, or catalytic upgrading, could enhance energy efficiency and decrease operational footprint. The development of heat recovery loops and energy integration is also crucial to lowering net energy consumption per unit WHC.

4.1.4. By-Product Streams and Environmental Management

HTC simultaneously produces gaseous (mainly CO_2, with small amounts of CH_4 and CO) and aqueous by-products (organic acids, sugars, phenolics, residual dissolved organics). Improper disposal or treatment can negate the environmental benefits of HTC.[105] Thorough characterization of gaseous and liquid effluents is crucial. Cleaner valorization options include CO_2 capture for use in electrocatalysis or CO_2-conversion batteries, as well as aqueous organics serving as feedstock for biogas production, fermentation, or chemical extraction.[106] Recycling or recirculating process water, after selective purification, can significantly reduce freshwater use. Reuse strategies must consider the accumulation of inhibitory species or salts over time.

4.1.5. Techno-Economic and Life Cycle Evaluation

Many studies focus heavily on material synthesis and electrochemical metrics, while neglecting comprehensive assessments of energy input, emissions, yield, and cost.[105] To properly justify the use of WHC-based devices, each process should be supported by a detailed techno-economic analysis (TEA) and a life-cycle assessment (LCA) in accordance with established standards (e.g., ISO 14 040).[107] These analyses need to include upstream biomass logistics, HTC operation, post-treatment, and subsequent recycling or disposal. Only by quantifying carbon footprints, net energy yields, and cost per kilowatt-hour can the true competitiveness of WHC electrodes be assessed.[105]

4.1.6. Feedstock-Tailored Optimization

Different biomass types (e.g., lignin-rich, cellulose-rich, agricultural residues, algae) respond differently under HTC.[108] The same HTC conditions may yield suboptimal char from one feedstock but excellent material from another. Systematic studies to explore parameter space (temperature, residence time, water ratio, catalysts) by feedstock class are required. In this context, machine learning and modelling approaches (e.g., regression, decision trees, neural networks) can accelerate parameter tuning and performance prediction. Recent efforts have indeed used ML to correlate feedstock and reaction variables to hydrochar yields and properties with high accuracy ($R^2 > 0.88$).[109]

4.1.7. Trade-Off Between Yield and Carbonization Degree

In HTC, there is a well-known trade-off: increasing severity (temperature or time) generally enhances carbonization and the development of graphitic structure, but it results in lower solid yields (producing more gas or liquid products).[110] This challenge complicates optimization, especially when aiming for both high yields and strong electrochemical stability. Strategies to address this include using catalysts or co-carbonization and co-hydrothermal approaches (e.g., co-HTC with other waste materials) to shift reaction equilibria favorably.[111]

4.2. Future Perspectives

To fully unlock the promise of HTC-derived WHC in sustainable energy storage, we propose the following strategic directions:

- Standardization and protocols: A working group or consortium could propose minimal reporting requirements for feedstock properties, HTC conditions, and electrochemical testing protocols. This level of standardization will accelerate cross-laboratory comparability and meta-analyses.[103]
- Biorefinery integration: HTC should be embedded in broader biorefinery concepts.[103] Coupling with anaerobic digestion, catalytic upgrading, or co-conversion of aqueous effluent can increase resource utilization and revenue streams.[112,113] For example, aqueous phase organics might be upgraded to chemicals, reducing wastewater disposal burdens.

- Engineering of WHC: To enhance WHC performance for LIBs, SIBs, and SCs, targeted modifications (heteroatom doping, edge functionalization, templated porosity, and compositing with metal oxides or conductive nanostructures) should be pursued.[114] The aim is to tailor pore size distribution, defect density, and surface wettability for optimal ion transport and electron conduction.
- Digitalization and data-driven optimization: Machine-learning, process simulation, and model-based control can be employed to efficiently explore the multidimensional HTC parameter space, forecast properties of WHC, and steer adaptive operational strategies. Hybrid empirical–mechanistic models can speed up scale-up.[109]
- Policy and incentives: Considering the circular economy target, advocating for supportive policies such as carbon credits, waste-to-energy subsidies, and procurement incentives for green electrode materials is vital.[115] Government-backed demonstration projects and pilot plants can help bridge the "valley of death" between lab research and industry adoption.[116]
- Closed-loop lifecycle and recycling strategies: From the outset, design WHC-based devices with end-of-life recovery in mind (e.g., retrievable carbon, electrode reuse). Combining LCA and recycling models can ensure that the entire lifecycle remains carbon-efficient and cost-effective.[117] It can also produce novel functional materials for further applications.

5. Conclusion

HTC has become a transformative and sustainable approach for converting biomass waste into high-quality carbon-based materials suitable for EES applications. This review critically explores the role of WHC in LIBs, SIBs, and SCs, emphasizing the benefits of HTC over traditional thermal conversion methods.

The two-step HTC followed by direct carbonization (HTC–DC) consistently showed better results than one-step DC, including higher carbon yields, greater porosity, customized surface functionalities, and improved electrochemical performance. WHC-based electrodes demonstrated promising specific capacities, ICE, and cycling stabilities across different feedstocks and device setups. Importantly, SIBs gained significantly from WHC's structural compatibility with sodium-ion storage, making HTC–DC a feasible option for next-generation, low-cost battery technologies. In supercapacitor applications, HTC-derived activated carbons achieved high surface areas and excellent capacitive properties, with long-term cycling stability. The HTC process also offers environmental and economic benefits, including reduced energy consumption, the elimination of drying steps, and the potential for integration with circular bioeconomy models. Despite these advances, several challenges persist, including feedstock variability, lack of standardized processing protocols, scalability constraints, and underutilized by-product management. Overcoming these issues through reactor innovation, lifecycle assessments, and the integration of hybrid systems will be vital for industrial uptake.

Overall, HTC offers a promising route to sustainable energy storage, allowing the conversion of biomass waste into functional materials with a lower carbon footprint. Future research should focus on understanding mechanisms, optimizing processes, and validating both technologically and economically to accelerate the transition from lab-based innovations to commercial use.

Acknowledgements

This research was funded by the Australian Department of Education through a Regional Research Collaboration (RRC) grant. This funding has allowed the establishment of the University of Southern Queensland-led SIMPLE Hub, where this research has been conducted. H.D.P. acknowledges the support of the University of Southern Queensland Early Career Researcher Program seed grant. AKN acknowledges funding in part from the Australian Research Council through the ARC Research Hub for Safe and Reliable Energy (SafeREnergy) – IH200100035 and the University of Southern Queensland (UniSQ) through a capacity-building program.

Conflict of Interest

The authors declare no conflict of interest.

Author Contributions

H.D.P. performed conceptualization, visualization, wrote the original draft, wrote, reviewed, and edited the final draft. T.S., A.K.N., and P.(P.)B. performed conceptualization, funding acquisition, wrote, reviewed, and edited. P.K.A. and J.F. wrote, reviewed, and edited; T.T.N. and A.H. conceptualization, wrote, reviewed, and edited.

Keywords

biomass valorization, hydrothermal carbonization, hydrochar, rechargeable batteries, supercapacitors

Received: July 31, 2025
Revised: October 2, 2025
Published online:

[1] R. Bonadiman, M. D. Lima, M. J. de Andrade, C. P. Bergmann, *J. Mater. Sci.* **2006**, *41*, 7288.
[2] M. J. Cao, S. D. Li, L. F. Nie, Y. F. Chen, *Mater. Today Sustain.* **2023**, *24*, 100522.
[3] H. Xu, H. Chen, C. Gao, *ACS Mater. Lett.* **2021**, *3*, 1221.
[4] B. J. Landi, M. J. Ganter, C. D. Cress, R. A. DiLeo, R. P. Raffaelle, *Energy Environ. Sci.* **2009**, *2*, 638.
[5] A. Pistone, C. Espro, *Curr. Opin. Green Sustain. Chem.* **2020**, *26*, 100374.
[6] H. D. Pham, K. Mahale, T. M. L. Hoang, S. G. Mundree, P. Gomez-Romero, D. P. Dubal, *ACS Appl. Mater. Interfaces* **2020**, *12*, 48518.
[7] Z. Xu, J. Wang, Z. Guo, F. Xie, H. Liu, H. Yadegari, M. Tebyetekerwa, M. P. Ryan, Y. S. Hu, M. M. Titirici, *Adv. Energy Mater.* **2022**, *12*, 2200208.
[8] M. Prieto, H. Yue, N. Brun, G. J. Ellis, M. Naffakh, P. S. Shuttleworth, *Polymers* **2024**, *16*, 2633.
[9] K. Kumar, R. Kumar, S. Kaushal, N. Thakur, A. Umar, S. Akbar, A. A. Ibrahim, S. Baskoutas, *Chemosphere* **2023**, *345*, 140419.
[10] Z. Zhang, S. Yang, H. Li, Y. Zan, X. Li, Y. Zhu, M. Dou, F. Wang, *Adv. Mater.* **2019**, *31*, 1805718.
[11] X. Zhu, Y. Zeng, X. Zhao, D. Liu, W. Lei, S. Lu, *EcoEnergy* **2025**, *3*, 70000.
[12] K. Nikgoftar, A. K. Madikere Raghunatha Reddy, M. V. Reddy, K. Zaghib, *Batteries* **2025**, *11*, 123.

[13] D. R. Lobato-Peralta, P. U. Okoye, C. Alegre, *J. Power Sources* **2024**, *617*, 235140.
[14] H. Duc Pham, C. Padwal, J. F. S. Fernando, T. Wang, T. Kim, D. Golberg, D. P. Dubal, *Batter. Supercaps* **2022**, *5*, 202100335.
[15] Z. Tang, R. Liu, D. Jiang, S. Cai, H. Li, D. Sun, Y. Tang, H. Wang, *ACS Appl. Mater. Interfaces* **2024**, *16*, 47504.
[16] J. Y. Hwang, S. T. Myung, Y. K. Sun, *Chem. Soc. Rev.* **2017**, *46*, 3529.
[17] S. Qiu, L. Meng, L. An, Q. Wu, S. Cui, Z. Hao, Y. Zhao, H. Zhang, *J. Energy Storage* **2025**, *132*, 117834.
[18] B. Zhong, C. Liu, D. Xiong, J. Cai, J. Li, D. Li, Z. Cao, B. Song, W. Deng, H. Peng, H. Hou, G. Zou, X. Ji, *ACS Nano* **2024**, *18*, 16468.
[19] H. Zhong, Q. Huang, M. Zou, F. Li, Y. Liu, Y. Luo, G. Ma, Y. Wu, X. Lin, L. Hu, *Chem. Eng. J.* **2025**, *508*, 160879.
[20] T. J. Yokokura, J. R. Rodriguez, V. G. Pol, *ACS Omega* **2020**, *5*, 19715.
[21] A. Singh, V. C. Srivastava, I. Janowska, *Energy Storage* **2024**, *6*, 677.
[22] S. Rajput, V. Tyagi, Sonika, R. N, S. K. Verma, *Energy Technol.* **2025**, *13*, 2401977.
[23] H. D. Pham, T. Shelley, P. P. Burey, J. Feldman, A. Helwig, *Biomass Bioenergy* **2025**, *201*, 108151.
[24] Y. Li, D. Xia, L. Tao, Z. Xu, D. Yu, Q. Jin, F. Lin, H. Huang, *ACS Appl. Mater. Interfaces* **2024**, *16*, 28461.
[25] S. Yu, J. He, Z. Zhang, Z. Sun, M. Xie, Y. Xu, X. Bie, Q. Li, Y. Zhang, M. Sevilla, M. M. Titirici, H. Zhou, *Adv. Mater.* **2024**, *36*, 2307412.
[26] M.-M. Titirici, R. J. White, C. Falco, M. Sevilla, *Energy Environ. Sci.* **2012**, *5*, 6796.
[27] M. Tariq, K. Ahmed, Z. Khan, M. P. Sk, *Chem. Asian J.* **2025**, *20*, 202500094.
[28] K. V. Supraja, T. R. K. C. Doddapaneni, P. K. Ramasamy, P. Kaushal, S. Z. Ahammad, K. Pollmann, R. Jain, *Chem. Eng. J.* **2023**, *473*, 145059.
[29] N. Nieto, J. Porte, D. Saurel, L. Djuandhi, N. Sharma, A. Lopez-Urionabarrenechea, V. Palomares, T. Rojo, *ChemSusChem* **2023**, *16*, 202301053.
[30] S. A. Nicolae, H. Au, P. Modugno, H. Luo, A. E. Szego, M. Qiao, L. Li, W. Yin, H. J. Heeres, N. Berge, M.-M. Titirici, *Green Chem.* **2020**, *22*, 4747.
[31] L. Wang, Z. Schnepp, M. M. Titirici, *J. Mater. Chem. A* **2013**, *1*, 5269.
[32] D. Alvira, D. Antorán, H. Darjazi, G. A. Elia, V. Sebastian, J. J. Manyà, *J. Power Sources* **2024**, *614*, 235043.
[33] E. Bevan, J. Fu, M. Luberti, Y. Zheng, *RSC Adv.* **2021**, *11*, 34870.
[34] S. Kang, X. Li, J. Fan, J. Chang, *Ind. Eng. Chem. Res.* **2012**, *51*, 9023.
[35] G. Ischia, M. Cutillo, G. Guella, N. Bazzanella, M. Cazzanelli, M. Orlandi, A. Miotello, L. Fiori, *Chem. Eng. J.* **2022**, *449*, 137827.
[36] M.-M. Titirici, M. Antonietti, N. Baccile, *Green Chem.* **2008**, *10*, 1204.
[37] R. P. Ipiales, M. A. de la Rubia, E. Diaz, A. F. Mohedano, J. J. Rodriguez, *Energy Fuels* **2021**, *35*, 17032.
[38] B. Zhang, B. K. Biswal, J. Zhang, R. Balasubramanian, *Chem. Rev.* **2023**, *123*, 7193.
[39] A. M. Smith, S. Singh, A. B. Ross, *Fuel* **2016**, *169*, 135.
[40] A. Picone, M. Volpe, W. Malik, R. Volpe, A. Messineo, *Biomass Bioenergy* **2024**, *181*, 107061.
[41] H. S. Kambo, A. Dutta, *Renew. Sustain. Energy Rev.* **2015**, *45*, 359.
[42] K. S. R. Judy A Libra, C. Kammann, M.-M. Titirici, C. Fühner, O. Bens, A. Funke, N. D. Berge, Y. Neubauer, J. Kern, K.-H. Emmerich, *Biofuels* **2011**, *2*, 89.
[43] Y. Wang, J. J. Wu, *Renew. Sustain. Energy Rev.* **2023**, *187*, 113754.
[44] N. Soltani, A. Bahrami, L. Giebeler, T. Gemming, D. Mikhailova, *Prog. Energy Combust. Sci.* **2021**, *87*, 100929.
[45] A. K. Mohanty, S. Vivekanandhan, O. Das, L. M. Romero Millán, N. B. Klinghoffer, A. Nzihou, M. Misra, *Nat. Rev. Methods Primers* **2024**, *4*, 19.
[46] B. Babinszki, E. Jakab, Z. Sebestyén, M. Blazsó, B. Berényi, J. Kumar, B. B. Krishna, T. Bhaskar, Z. Czégény, *J. Anal. Appl. Pyrolysis* **2020**, *149*, 104844.
[47] A. F. Qatarneh, C. Dupont, J. Michel, L. Simonin, A. Beda, C. Matei Ghimbeu, V. Ruiz-Villanueva, D. da Silva, H. Piégay, M. J. Franca, *J. Environ. Chem. Eng.* **2021**, *9*, 106604.
[48] Z. Wang, X. Zhang, X. Liu, Y. Zhang, W. Zhao, Y. Li, C. Qin, Z. Bakenov, *J. Colloid Interface Sci.* **2020**, *569*, 22.
[49] C. Zhao, J. Luo, Z. Hu, *Micro Nano Lett.* **2018**, *13*, 1386.
[50] E. C. Oskaras Alšauskas, M. Huismans, E. Jenness, J. Jorquera Copier, J.-B. Le Marois, T. Lombardo, S. McDonagh, V. O'Riordan, A. Petropoulos, Jules Sery, IEA, IEA, **2024**, p. 174.
[51] L. Zhu, B. Luo, L. Men, J. Chen, F. Xie, W. Zhang, J. Zhang, Y. Zhou, *Green Chem.* **2025**, *27*, 2078.
[52] Y. Li, A. Vasileiadis, Q. Zhou, Y. Lu, Q. Meng, Y. Li, P. Ombrini, J. Zhao, Z. Chen, Y. Niu, X. Qi, F. Xie, R. van der Jagt, S. Ganapathy, M.-M. Titirici, H. Li, L. Chen, M. Wagemaker, Y.-S. Hu, *Nat. Energy* **2024**, *9*, 134.
[53] J. Cui, P. Su, W. Li, X. Wang, Y. Zhang, Z. Xiao, Q. An, Z. Chen, *Adv. Energy Mater.* **2025**, *15*, 2404604.
[54] S. Alvin, H. S. Cahyadi, J. Hwang, W. Chang, S. K. Kwak, J. Kim, *Adv. Energy Mater.* **2020**, *10*, 2000283.
[55] A. K. Nanjundan, R. R. Gaddam, A. H. F. Niaei, P. K. Annamalai, D. P. Dubal, D. J. Martin, Y. Yamauchi, D. J. Searles, X. S. Zhao, *Batter. Supercaps* **2020**, *3*, 953.
[56] R. A. Afzal, P. K. Annamalai, M. Tebyetekerwa, P. Burey, J. Bell, A. K. Nanjundan, D. J. Martin, *RSC Sustain.* **2025**, *3*, 1691.
[57] S. Manna, S. Puravankara, *J. Power Sources* **2025**, *647*, 237335.
[58] S. K. Saju, S. Chattopadhyay, J. Xu, S. Alhashim, A. Pramanik, P. M. Ajayan, *Cell Rep. Phys. Sci.* **2024**, *5*, 101851.
[59] L. F. Zhao, Z. Hu, W. H. Lai, Y. Tao, J. Peng, Z. C. Miao, Y. X. Wang, S. L. Chou, H. K. Liu, S. X. Dou, *Adv. Energy Mater.* **2021**, *11*, 2002704.
[60] Y. Li, Y. Lu, P. Adelhelm, M. M. Titirici, Y. S. Hu, *Chem. Soc. Rev.* **2019**, *48*, 4655.
[61] H. Kim, J. C. Hyun, D. H. Kim, J. H. Kwak, J. B. Lee, J. H. Moon, J. Choi, H. D. Lim, S. J. Yang, H. M. Jin, D. J. Ahn, K. Kang, H. J. Jin, H. K. Lim, Y. S. Yun, *Adv. Mater.* **2023**, *35*, 2209128.
[62] Y. Nishi, *Chem. Rec.* **2001**, *1*, 406.
[63] O. Fromm, A. Heckmann, U. C. Rodehorst, J. Frerichs, D. Becker, M. Winter, T. Placke, *Carbon* **2018**, *128*, 147.
[64] M. Inagaki, F. Kang, *Materials Science and Engineering of Carbon: Fundamentals*, 2nd ed., Butterworth-Heinemann, Oxford UK **2014**.
[65] P. Engels, F. Cerdas, T. Dettmer, C. Frey, J. Hentschel, C. Herrmann, T. Mirfabrikikar, M. Schueler, *J. Clean. Prod.* **2022**, *336*, 130474.
[66] W. Long, B. Fang, A. Ignaszak, Z. Wu, Y. J. Wang, D. Wilkinson, *Chem. Soc. Rev.* **2017**, *46*, 7176.
[67] E. Unur, S. Brutti, S. Panero, B. Scrosati, *Microporous Mesoporous Mater.* **2013**, *174*, 25.
[68] M. Curcio, S. Brutti, L. Caripoti, A. De Bonis, R. Teghil, *Nanomaterials* **2021**, *11*, 3183.
[69] Z. Guo, Z. Xu, F. Xie, J. Jiang, K. Zheng, S. Alabidun, M. Crespo-Ribadeneyra, Y. S. Hu, H. Au, M. M. Titirici, *Adv. Mater.* **2023**, *35*, 2304091.
[70] L. Wang, J. Xue, B. Gao, P. Gao, C. Mou, J. Li, *RSC Adv.* **2014**, *4*, 64744.
[71] L. Fan, L. Fan, T. Yu, X. Tan, Z. Shi, *Int. J. Electrochem. Sci.* **2020**, *15*, 1035.
[72] K. Yu, J. Wang, K. Song, X. Wang, C. Liang, Y. Dou, *Nanomaterials* **2019**, *9*, 93.
[73] C. Padwal, H. D. Pham, L. T. M. Hoang, S. Mundree, D. Dubal, *Sustain. Mater. Technol.* **2023**, *35*, 00547.
[74] G. Huang, H. Zhang, F. Gao, D. Zhang, Z. Zhang, Y. Liu, Z. Shang, C. Gao, L. Luo, M. Terrones, Y. Wang, *Carbon* **2024**, *228*, 119354.
[75] S. Sarkar, S. Roy, Y. Hou, S. Sun, J. Zhang, Y. Zhao, *ChemSusChem* **2021**, *14*, 3693.

[76] D. S. Premathilake, W. A. M. A. N. Illankoon, A. B. Botelho Junior, C. Milanese, J. A. S. Tenório, D. C. R. Espinosa, M. Vaccari, *ACS Sustain. Chem. Eng.* **2025**, *13*, 1737.
[77] X. Wei, Z. Guo, Y. Zhao, Y. Sun, A. Hankin, M. Titirici, *RSC Sustain.* **2025**, *3*, 264.
[78] N. Nieto, O. Noya, A. Iturrondobeitia, P. Sanchez-Fontecoba, U. Pérez-López, V. Palomares, A. Lopez-Urionabarrenechea, T. Rojo, *Batteries* **2022**, *8*, 28.
[79] R. Li, J. Huang, Z. Xu, H. Qi, L. Cao, Y. Liu, W. Li, J. Li, *Energy Technol.* **2018**, *6*, 1080.
[80] Y. Li, S. Xu, X. Wu, J. Yu, Y. Wang, Y.-S. Hu, H. Li, L. Chen, X. Huang, *J. Mater. Chem. A* **2015**, *3*, 71.
[81] H. Au, H. Alptekin, A. C. S. Jensen, E. Olsson, C. A. O'Keefe, T. Smith, M. Crespo-Ribadeneyra, T. F. Headen, C. P. Grey, Q. Cai, A. J. Drew, M.-M. Titirici, *Energy Environ. Sci.* **2020**, *13*, 3469.
[82] L. Cong, G. Tian, D. Luo, X. Ren, X. Xiang, *J. Electroanal. Chem.* **2020**, *871*, 114249.
[83] D. Alvira, D. Antorán, H. Darjazi, G. A. Elia, C. Gerbaldi, V. Sebastian, J. J. Manyà, *J. Mater. Chem. A* **2025**, *13*, 2730.
[84] J. Wang, L. Yan, Q. Ren, L. Fan, F. Zhang, Z. Shi, *Electrochim. Acta* **2018**, *291*, 188.
[85] Z. X. Fei Xie, A. C. S. Jensen, F. Ding, H. Au, J. Feng, H. Luo, Mo Qiao, Z. Guo, Y. Lu, A. J. Drew, Y.-S. Hu, M.-M. Titirici, *J. Mater. Chem. A* **2019**, *7*, 27567.
[86] W. Li, J. Cui, W. Ye, P. Su, X. Song, T. Yang, Y. Zhang, Z. Chen, *J. Mater. Chem. A* **2025**, *13*, 18388.
[87] D. P. Dubal, J. Suarez-Guevara, D. Tonti, E. Enciso, P. Gomez-Romero, *J. Mater. Chem. A* **2015**, *3*, 23483.
[88] Y. Wang, L. Zhang, H. Hou, W. Xu, G. Duan, S. He, K. Liu, S. Jiang, *J. Mater. Sci.* **2020**, *56*, 173.
[89] M. Prieto, G. J. Ellis, V. Budarin, E. Morales, M. Naffakh, P. S. Shuttleworth, *J. Mater. Chem. A* **2024**, *12*, 29698.
[90] N. Ahmad, A. Rinaldi, M. Sidoli, G. Magnani, V. Vezzoni, S. Scaravonati, L. Pasetti, L. Fornasini, H. Gupta, M. Tamagnone, F. Ridi, C. Milanese, M. Riccò, D. Pontiroli, *J. Power Sources* **2024**, *624*, 235511.
[91] A. Jain, R. Balasubramanian, M. P. Srinivasan, *Chem. Eng. J.* **2016**, *283*, 789.
[92] B. K. Saikia, S. M. Benoy, M. Bora, J. Tamuly, M. Pandey, D. Bhattacharya, *Fuel* **2020**, *282*, 118796.
[93] L. Wei, M. Sevilla, A. B. Fuertes, R. Mokaya, G. Yushin, *Adv. Energy Mater.* **2011**, *1*, 356.
[94] G. Sun, L. Qiu, M. Zhu, K. Kang, X. Guo, *Ind. Crops Prod.* **2018**, *125*, 41.
[95] N. Yadav, M. K. Singh, N. Yadav, S. A. Hashmi, *J. Power Sources* **2018**, *402*, 133.
[96] J. Zhang, Z. Chen, G. Wang, L. Hou, C. Yuan, *Appl. Surf. Sci.* **2020**, *533*, 147511.
[97] Y. Liu, B. Huang, X. Lin, Z. Xie, *J. Mater. Chem. A* **2017**, *5*, 13009.
[98] X. Wang, S. Yun, W. Fang, C. Zhang, X. Liang, Z. Lei, Z. Liu, *ACS Sustainable Chem. Eng.* **2018**, *6*, 11397.
[99] Y. Fan, P. Liu, B. Zhu, S. Chen, K. Yao, R. Han, *Int. J. Hydrogen Energy* **2015**, *40*, 6188.
[100] L. Shi, L. Jin, Z. Meng, Y. Sun, C. Li, Y. Shen, *RSC Adv.* **2018**, *8*, 39937.
[101] L. Peng, Y. Liang, H. Dong, H. Hu, X. Zhao, Y. Cai, Y. Xiao, Y. Liu, M. Zheng, *J. Power Sources* **2018**, *377*, 151.
[102] S. Shekoohiyan, A. Sajadi, G. Moussavi, M. Heidari, *Int. J. Environ. Sci. Technol.* **2025**, *22*, 8335.
[103] M. Heidari, A. Dutta, B. Acharya, S. Mahmud, *J. Energy Inst.* **2019**, *92*, 1779.
[104] T.-T. Ho, A. Nadeem, K. Choe, *Energies* **2024**, *17*, 1918.
[105] M. Cavali, A. P. Dresch, I. M. Belli, N. Libardi Junior, A. L. Woiciechowski, S. R. Soares, A. B. Castilhos Junior, *J. Clean. Prod.* **2025**, *491*, 144838.
[106] R. V. P. Antero, A. C. F. Alves, S. B. de Oliveira, S. A. Ojala, S. S. Brum, *J. Clean. Prod.* **2020**, *252*, 119899.
[107] A. Saba, K. McGaughy, M. Reza, *Energies* **2019**, *12*, 630.
[108] M. Akbari, A. O. Oyedun, A. Kumar, *Bioresour. Technol. Rep.* **2019**, *7*, 100210.
[109] A. Shafizadeh, H. Shahbeik, S. Rafiee, A. Moradi, M. Shahbaz, M. Madadi, C. Li, W. Peng, M. Tabatabaei, M. Aghbashlo, *Fuel* **2023**, *347*, 128467.
[110] X. Luo, X. Pei, X. Zhang, H. Du, L. Ju, S. Li, L. Chen, J. Zhang, *Environ. Res.* **2025**, *270*, 121023.
[111] J. Gao, Q. Wang, C. Yin, J. Su, C. Cao, J. Duo, P.-G. Duan, *Biomass Bioenergy* **2025**, *202*, 108164.
[112] F. Williams, P. Harris, S. Tait, B. S. Mickan, W. Merkle, H. J. Nagele, B. K. McCabe, *Waste Manag.* **2025**, *208*, 115153.
[113] A. Rehman, M. Park, S.-J. Park, *Coatings* **2019**, *9*, 103.
[114] T. N. Ang, B. R. Young, R. Burrell, M. Taylor, M. K. Aroua, S. Baroutian, *Chemosphere* **2021**, *264*, 128535.
[115] B. Krieger, V. Zipperer, *Res. Policy* **2022**, *51*, 104516.
[116] Y. Zhai, X. Huang, *Nexus* **2024**, *1*, 100032.
[117] X. Luo, X. Pei, X. Zhang, T. Hu, T. Liu, *Chem. Eng. J.* **2025**, *524*, 168500.

David (Hong Duc) Pham is a postdoctoral research fellow (Novel Energy Technologies) at SIMPLE Hub, Centre for Future Materials, University of Southern Queensland. He obtained his PhD from Queensland University of Technology in 2020 and joined UniSQ in 2023. His research focuses on waste upcycling, carbonisation, renewable energy, low-carbon liquid fuels, and electrochemical energy storage.

Tristan Shelley is an experienced project leader of industry-focused R&D programs, provides advice for the strategic direction of the Centre for Future Materials, and is a technical specialist in advanced composites manufacturing technologies. Dr Shelley's specialisation focuses on advanced manufacturing of composite materials and accelerated processing techniques, including bonding and joining of aerospace structures. Areas of technical experience and knowledge range from filament winding, numerical modelling, structural design, and numerous composite manufacturing techniques and characterisation methods.

Paulomi (Polly) Burey is a Professor at the Centre for Future Materials, University of Southern Queensland and co-Director of SIMPLE Hub. Dr Burey is a chemical and materials engineer/food scientist with expertise in developing a fundamental understanding of the relationships between formulation, microstructure, processing and rheological behaviour of food (and other!) materials. Dr Burey has over 20 years of experience working on industry-linked research.

Ashok Kumar Nanjunda, FRSC is a Professor of Energy Storage at the University of Southern Queensland (UniSQ), Australia, and a Fellow of the Royal Society of Chemistry. England. A nanomaterials and energy expert, he formerly served as Chief Scientific Officer of a publicly listed graphene company, integrating academic research with industrial innovation. A recipient of the Marie-Curie, JSPS-Japan, and UQ Fellowships, his work focuses on carbon nanostructures and sustainable battery technologies. With over 100 publications and seven patents in journals including Chemical Reviews, Advanced Functional Materials, and Nature Protocols (h-index 55), he is globally recognised for advancing next-generation energy storage and mentoring future innovators. Prof. Nanjundan currently leads the clean energy research portfolio at the Centre for Future Materials at UniSQ.